Observations of Thermally Developed Wind Systems in Mountainous Terrain

C. DAVID WHITEMAN

Pacific Northwest Laboratory, Richland, Washington

ABSTRACT

Slope and valley wind systems are local thermally driven circulations that form frequently in complex terrain areas. Recent research has focused on the temperature structure along the slope and valley axes that leads to the wind systems. Two new tools being used in these analyses include the topographic amplification factor, which quantifies the role of the topography in producing bulk temperature gradients along a valley's axis, and atmospheric heat budgets, which identify key physical processes leading to changes in temperature structure. Both tools are in an early stage of development, are being applied primarily to steady-state nighttime periods, and are leading to new concepts and understanding.

Recent climatological evidence in Austria's Inn Valley and in several Colorado valleys supports the concept that valley winds are driven by horizontal pressure gradients that are built up hydrostatically by the changing temperature structure along a valley's length. Topographic amplification factors appear to be useful in assessing the strength of valley wind systems. Several components of valley atmospheric heat budgets have proven difficult to measure, and large imbalances are being experienced. Several recent experiments, in a range of climatological regimes, suggest that measured nighttime surface sensible heat fluxes are too small to result in balances. This may be caused by measurement errors or by nonrepresentative measurements. The advective and radiative flux divergence components are also uncertain.

A simple conceptual model of diurnal wind and temperature structure evolution in deep valleys is presented. During the morning transition period, upslope flows form over heated valley sidewalls and compensatory subsidence over the valley center produces warming that eventually reverses the down-valley winds. The key role of vertical motions in transferring energy through the valley atmosphere during the morning transition period has been demonstrated by field and modeling studies.

The evening transition period has received little observational attention, and the key physical processes are not yet well known. Investigation of slope wind systems has focused mostly on the nighttime flows. Flows on the sides of isolated mountains are reasonably well understood when external flows are weak, but slope flows on valley sidewalls are complicated by the continued evolution of temperature structure within the valley and the strong influence of the overlying along-valley flows.

Recent experiments have shown that thermally driven flows within the topography may be influenced in subtle ways by the overlying circulations. This influence is nearly always present to some extent, but has not yet been systematically investigated. Recent research on strong winds that issue from a valley's exit at night and on tributary flows is briefly summarized, and some comments are made on Maloja winds and antiwind systems. The chapter ends with a summary of topics needing further research.

2.1. Introduction to diurnal mountain winds

Two classifications of diurnal mountain wind systems are generally recognized (Fig. 2.1). *Slope winds* blow parallel to the inclination of the sidewalls and are called upslope and downslope winds. The slope winds are produced by buoyancy forces induced by temperature differences between the air adjacent to the slope and the ambient air outside the slope boundary layer. Typically, slope winds blow up the slope by day and down the slope by night. *Valley winds* blow parallel to the longitudinal axis of a valley. These winds are produced by horizontal pressure gradients that develop as a result of temperature differences that form along the valley axis or temperature differences between the air in the valley and the air at the same height over the adjacent plain. Valley winds typically blow up-valley during daytime and down-valley during nighttime, although their onset can be substantially delayed in valleys where large atmospheric volumes are involved. A variety of names have been applied to these wind systems, with usage varying somewhat from country to country. Alternative terminology for the diurnal mountain winds is listed in Table 2.1.

Study of the pure thermally developed winds is complicated by the influence of other wind systems that develop on different scales, of regional pressure gradients superimposed on the topography, and of mechanical effects induced by the topography on the wind systems themselves or on overlying wind systems. In this chapter, we emphasize thermally developed wind systems, and these complications will be considered as modifying influences.

Increases in understanding of slope and valley wind systems in the last decade have come from the combined efforts of observationalists, theoreticians, and modelers. This chapter deals primarily with observations of ther-

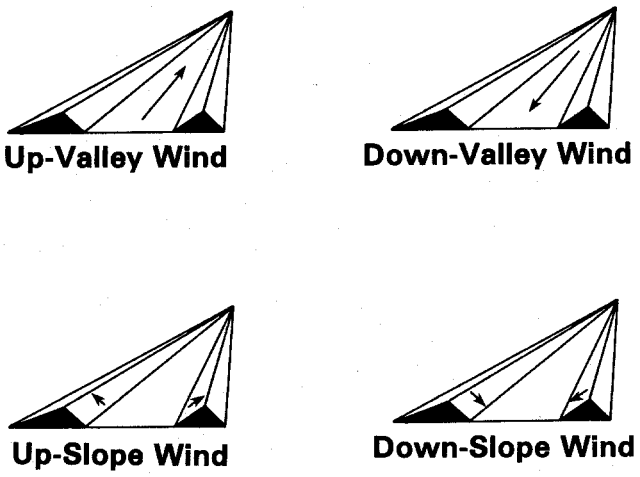

FIG. 2.1. Wind system terminology.

mally developed wind systems, and the reader is assumed to have some general knowledge concerning the structure of valley and slope wind systems and wind system research through the 1970s. Prior reviews of these topics are listed in Table 2.2. Insights into theory and modeling are presented by Egger, Chapter 3.

In this chapter we summarize recent observations of along-valley and along-slope wind systems and their interactions, new findings on the morning and evening transition periods when the wind systems are reversed, and provide an overall view of the diurnal evolution of temperature and wind structure in deep valleys. The paper concludes with several peripheral topics, and points out the needs for future research.

2.1.1. *Summary of recent field experiments*

A partial list of complex terrain meteorology field experiments conducted in the last 10 years is provided in Tables 2.3 and 2.4. Most experiments have taken place during short campaigns that lasted typically 1 or 2 weeks during summer or fall and were intended to investigate well-developed circulations in simple topography during clear, undisturbed weather conditions. Relatively few experiments were conducted in winter or in large valley-ridge complexes, and few experiments were focused on developing long-term climatologies of local circulations. Finally, most field studies have been concerned with mean flows, so that little information is yet available on turbulent fluctuations or wave motions.

Manins and Sawford (1979a) summarized data on downslope winds by stating that "the data are almost all confined to wind fields and only rarely is information about their spatial and temporal variation included. Practically no temperature data are available." Their statement could also be fairly applied to valley wind systems in general. In the last 10 years, however, new instruments have become more widely used, including commercial tethered balloon systems, portable upper-air sounding systems, instrumented aircraft (including motorgliders), atmospheric tracer systems, and remote sensors such as Doppler sodars and Doppler lidars. Temperature data are now collected routinely, along with wind data. A current review of remote sensing technology as applied to complex terrain meteorology is presented by Neff, Chapter 8.

In many cases, different instrument systems have been used by American and European experimenters. Motorgliders, for instance, have been used extensively in the European experiments but have never been used in U.S. experiments. Tracer experiments and new remote sensing

TABLE 2.1. Alternative names for thermally driven wind systems in valleys.

	Wind			
	Downslope	Down-valley	Upslope	Up-valley
Generic terms				
Thermal winds	×	×	×	×
Topographic winds	×	×	×	×
Valley winds	×	×	×	×
Mountain winds	×	×	×	×
Thermally driven winds	×	×	×	×
Valley winds		×		×
Valley wind (German, Talwind)				×
Mountain wind (German, Bergwind)		×		
In-valley wind (German, Taleinwind)				×
Out-valley wind (German, Talauswind)		×		
Ascending valley wind				×
Descending valley wind		×		
Slope winds				
Katabatic wind	×			
Anabatic wind			×	
Mixed terms				
Gravitation wind	×	×		
Drainage wind	×	×		
Night wind	×	×		
Day wind			×	×

TABLE 2.2. Previous reviews of mountain meteorology literature.

Author	Description
Hawkes (1947)	Good English summary of historical Alpine work.
Defant (1949)	Summary of Wagner's theory and interrelationship between slope and valley wind systems (in German).
Defant (1951)	English summary of portions of Defant (1949) and summary of other thermally developed circulations, including sea breezes, glacier winds, etc.
Brooks (1951)	Summary of mountain meteorology research, focusing on work published in English.
Geiger (1965)	Microclimatology text.
Yoshino (1975)	Updated microclimatology text.
Barr et al. (1977)	Summary of research needs in complex terrain meteorology focused on energy development activities.
Smith (1979)	Influence of mountains on the earth's atmosphere, focus on large scales of motion.
Atkinson (1981)	Summary of observational and theoretical work on slope and valley wind systems.
Orgill (1981)	Broad summary of mountain effects and results of a search for U.S. experimental areas.
Barry (1981)	Mountain meteorology textbook, focus on broad range of mountain effects.
Whiteman and Dreiseitl (1984)	Translation of classical German and French papers on theory of slope and valley flows. Summary of recent European field experiments.
Pielke (1984)	Modeling of mesoscale atmospheric processes.

tools, on the other hand, have been used predominantly in the United States. Studies have focused on a range of phenomena on different spatial scales, investigating katabatic flows on isolated hillsides, locally developed circulations in small well-defined valleys, and the meteorology of large valley complexes, especially in the Alps. The major experiments have utilized increasing resources and become logistically quite complicated, involving many collaborators. The result has been intensive experiments and large databases for a small number of valleys. These databases have been useful for the development and testing of dynamic models.

There is an increasing recognition among researchers that the valley meteorology problem is a continuum problem. While the physical processes affecting the circulations can be identified, the relative importance of the different processes varies from valley to valley, from time to time in the same valley, and even from segment to segment along a valley's length. The continuum in topographic complexity and scale, above-valley flows, climate, valley energy budgets, and even the scales of the local circulations, ensures that generalizations will be difficult. New tools and techniques are increasingly applied to address these continuum problems, however. Combined efforts by modelers and observationalists to design appropriate field experiments, and systematic model simulations in which different boundary conditions are imposed (e.g., terrain, surface energy budgets, and external ambient wind fields) seem particularly promising.

2.2. Along-valley wind systems

According to Wagner (1932a, 1938), along-valley wind systems are the result of a greater diurnal temperature range in a vertical column within the valley than in a similar column with its base at the same elevation outside the valley. The differing diurnal temperature ranges produce a thermally developed, diurnally varying pressure gradient that drives the valley wind system (Fig. 2.2). Recent climatological evidence that supports Wagner's theory is presented next, followed by a discussion of the basic physical processes that produce the along-valley wind system, with emphasis placed on the important role of topography.

2.2.1. Climatology

A key question regarding thermally developed circulations in complex terrain is the frequency with which such circulations appear in seasonal or long-term averages. Perhaps the most detailed published climatology of a single valley is for Austria's Inn Valley. There, Nickus and Vergeiner (1984) investigated the diurnal course of horizontal pressure gradients between the valley (Innsbruck) and the adjacent plain (Munich) as a function of season on sunny days. They found (Fig. 2.3) a regular diurnal reversal of the valley-plain pressure gradient in all seasons except winter, with pressure gradients supporting up-valley winds during daytime and down-valley winds during nighttime, in conformance with theory. The peak daytime pressure gradient typically occurred at 1500 UTC in all seasons. The thermal forcing of the pressure gradients is clearly seen in Fig. 2.4. At all altitudes within the valley the diurnal temperature range was larger than the corresponding temperature range over the plain. Further, the diurnal temperature range increased with up-valley distance (Table 2.5). At Landeck, 156 km up the valley, the diurnal temperature range had attained 3.6 times the range over the adjacent plain just beyond the valley's mouth at Rosenheim. The Inn Valley's wind system, as measured at

TABLE 2.3. Major valley meteorology field experiments in the last decade.

Experiment	Experimental dates	Key references
HangWindExperiment Innsbruck (HAWEI).	29 Sept–16 Oct 1978	Freytag and Hennemuth (1979)
Experiments focused on the slopes of a major, deep Alpine valley in the interior of the Alps. Inn Valley, Austria.		Vergeiner (1983)
Das Mesoskalige KlimaProgramm im Oberrheintal (MESOKLIP).	17–28 Sept 1979	Fiedler and Prenosil (1980)
Experiments in a wide, shallow valley flowing north from the Alps. Rhine Valley, FRG.		
DISKUS.	6–15 Aug 1980	Freytag and Hennemuth (1981)
Experiments in an idealized, medium-sized tributary or end valley of the Alps. Dischma Valley, Switzerland.		Freytag and Hennemuth (1982)
		Reiter et al. (1981)
Mesoskaliges Experiment im Raum Kufstein/Rosenheim (MERKUR).	23 Mar–5 Apr 1982	Freytag and Hennemuth (1983)
Experiments in a mesoscale region centered on a major, deep interior Alpine valley. Inn Valley, Austria/FRG.		Reiter et al. (1982)
		Reiter et al. (1984)
Atmospheric Studies in Complex Terrain (ASCOT).	16–28 Jul 1979	Dickerson and Gudiksen (1984)
	11–25 Sept 1980	Orgill and Schreck (1985)
	12–24 Aug 1981	Clements et al. (1989a)
	26 Jul–8 Aug 1982	Special 1989 ASCOT JAM
	17 Sept–6 Oct 1984	issues (June and July 1989).
Experiments (1979 and 1980) in a valley basin on east side of coastal mountains in California. Experiments in 1981 in a V-shaped California valley draining west from coastal range. Experiments in Colorado (1982 and 1984) in an idealized semiarid end valley of the Rocky Mountains. Anderson Creek valley, CA; Big Sulfur Creek valley, CA; Brush Creek valley, CO.		ASCOT report series

TABLE 2.4. Other valley meteorology field experiments in the last decade.

Experimental program	Key references
Latrobe Valley, Australia 1975, 1978	Manins and Sawford (1979a, 1979b, 1982)
NSF/CSU program of T. B. McKee 1975–present	Whiteman (1982)
	Bader et al. (1987)
South Park, CO 1977	Banta (1984, 1985, 1986)
	Banta and Cotton (1981)
Innsbruck Research Program 1979–1983	Vergeiner (1983)
	Vergeiner and Dreiseitl (1987)
Pajarito Mountain, NM 1979	Clements and Nappo (1983)
Rattlesnake Mountain, WA 1980, 1981	Horst and Doran (1982, 1983, 1986, 1988)
	Doran and Horst (1983)
LOWEX III 1981	Müller et al. (1982)
	Reiter et al. (1983)
Japanese valleys	Sato and Kondo (1988)
	Kondo and Sato (1988)
First Himalaya Soaring Expedition 1985	Neininger and Reinhardt (1986)
U. of Wyoming 1985	Kelly (1988)
ROMPEX 1985	Reiter et al. (1987)
Aare Valley, Switzerland 1985–1986	Filliger et al. (1987)
Touchet Valley, WA 1986	Doran et al. (1989)
Frijoles Canyon, NM 1987	Stone and Hoard (1989)
ASCOT Colorado valleys 1988	yet unpublished

the Innsbruck Meteorological Institute and on a 200-m-high isolated hill (Berg Isel) above the floor of the valley near Innsbruck, was consistent with the pressure gradients (Figs. 2.5 and 2.6). Wind system onset and cessation times varied throughout the year in agreement with the supposed thermal forcing. Up-valley winds were strongest in mid-afternoon, attaining mean values of nearly 4 m s^{-1} in

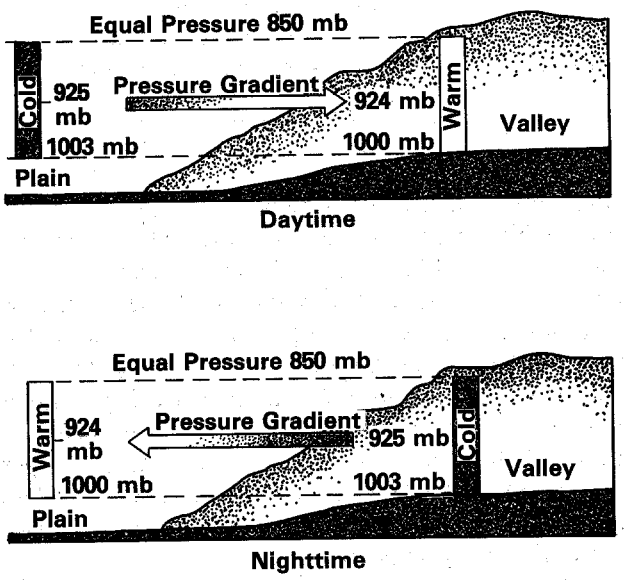

FIG. 2.2. Illustration of the thermal forcing of valley-plain pressure gradients leading to the development of an along-valley wind system. (Adapted from Hawkes 1947.)

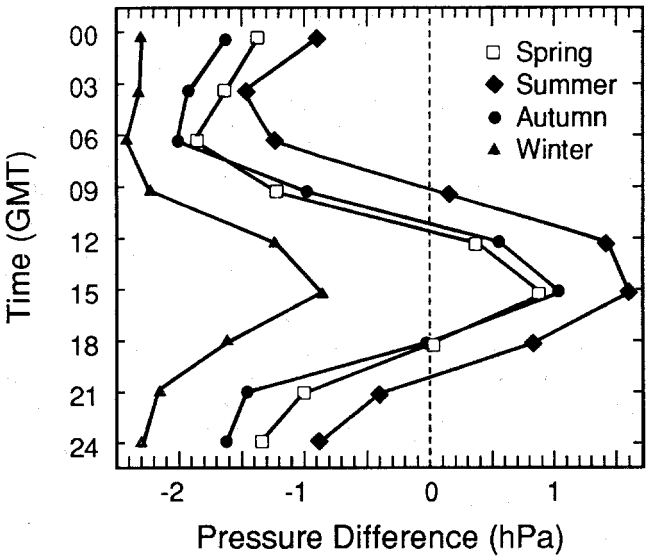

FIG. 2.3. Daily march of horizontal pressure gradient at 550 m MSL between a plain station (Munich) and a deep valley station (Innsbruck), sunny days. (Nickus and Vergeiner 1984.)

summer and fall. Down-valley winds attained mean values larger than 7 m s^{-1} in winter at Berg Isel and persisted nearly the entire day, in agreement with the sign of the calculated pressure gradients. Further, the development

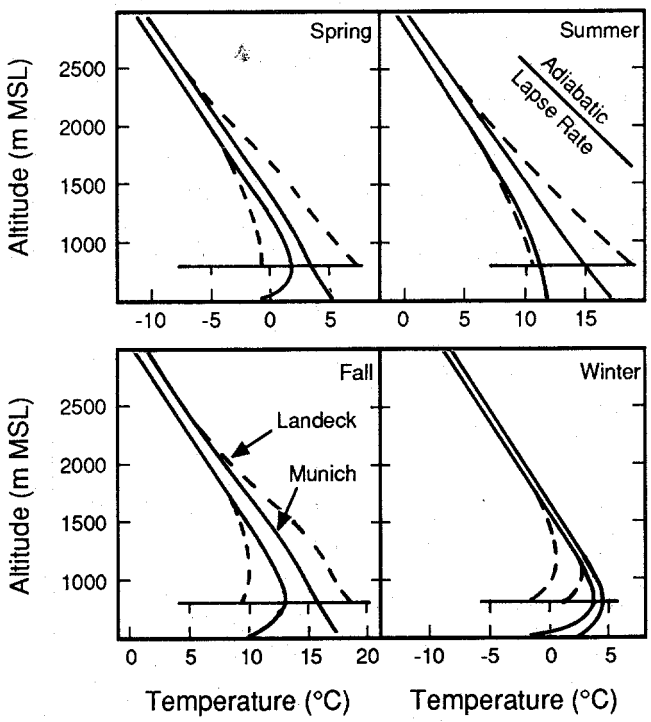

FIG. 2.4. Schematic vertical temperature profiles for a valley site (dashed line, Landeck, 821 m MSL in the Inn Valley) and for a site on the adjacent plain (solid curves, Munich, 529 m MSL) at 0600 and 1500 UTC, for all seasons. (Adapted from Nickus and Vergeiner 1984.)

of the local wind system depended on the synoptic weather type (Table 2.6). To investigate this dependence, Vergeiner (1983) stratified days according to the direction of the prevailing synoptic flow above the valley and determined whether the local wind system was evident on these days. At the Innsbruck Meteorological Institute and on the Berg Isel, valley winds were evident on 29% and 40% of the days of the year, respectively. In a smaller tributary to the Inn Valley (the Wipp valley) at Zenzenhof, valley winds occurred on 53% of the days. Near the valley exit at Kufstein, 60 km below Innsbruck, valley winds occurred on 32% of the days. Valley winds were most frequent on days with high pressure and weak synoptic winds.

The frequency of occurrence of valley wind days appears to be higher in continental areas of the western United States than in the Inn Valley, although direct comparison between published climatologies is difficult because of the differing definitions of valley wind days. In California's Anderson Creek valley, a relatively dry valley in the California coastal range that is subject to frequent marine intrusions, Gudiksen and Walton (1981) found strong monthly variations in drainage flow frequencies, with frequencies below 20% in February and March, 85% in August, and averaging 44% for the 10-month period investigated (Fig. 2.7). Colorado's semiarid Brush Creek valley, in the central Rocky Mountains, has well-defined valley wind circulations on more than 40% of the days in all months (Fig. 2.8), and in many months has valley winds on more than 60% of the days (Gudiksen 1989).

Climatological evidence thus supports Wagner's concept that valley wind circulations are driven by horizontal pressure gradients that are built up hydrostatically between valley and plain. (Nonhydrostratic flows may be significant in some cases, see Paegle et al., Chapter 10.) The pressure gradients produce a wind directed into the valley during the day when the valley column is warmer than the plain column, and directed out of the valley during the night when the valley column is colder. Pressure differences of several hPa in a distance of, say, 100 km (Fig. 2.2) may be considered typical of a very deep valley, with correspondingly smaller gradients in more shallow valleys. These thermally developed pressure gradients are comparable to typical synoptic scale pressure gradients, providing an explanation for the high climatological frequency of occurrence of the local circulations.

2.2.2. Basic physics

2.2.2.1. TOPOGRAPHIC AMPLIFICATION FACTOR

The diurnal reversal of the along-valley wind system arises from the larger diurnal temperature range in the valley atmosphere compared to the plains atmosphere.

TABLE 2.5. Daily ranges of valley mean temperature in the Inn Valley (Vergeiner and Dreiseitl 1987).

Station	Elevation (m)	Up-Valley distance (km)	Temperature range (1500–0600 UTC, °C)	Ratio with Rosenheim
Rosenheim	455	−17	1.7	1.0
Kufstein	508	15	3.0	1.8
Innsbruck	579	83	5.2	3.0
Landeck	821	156	6.1	3.6

This occurs as a consequence of the first and second laws of thermodynamics, expressed as

$$Q = \rho c_p V(T/\theta)d\theta. \tag{2.1}$$

Following this equation, a given increment of heat Q added to or subtracted from an atmospheric volume will produce a potential temperature change $d\theta$ in proportion to air density ρ, specific heat c_p, and volume $V(T/\theta$, the ratio of actual temperature to potential temperature, is near unity and is defined as $(p/p_0)^{R/cp}$, where p is atmospheric pressure, p_0 is atmospheric pressure at sea level, and R is the gas constant). The smaller the volume, the larger the potential temperature change for the same heat increment.

Applying this concept to the valley atmosphere, suppose that solar radiation enters a valley through the horizontal area at the top of the valley at ridgetop level and that, over the adjacent plain, solar radiation streams across an equivalent area at the same altitude. Assume further that the insolation, when received at the ground and converted to sensible heat flux, will heat the air below the horizontal areas, and we consider the elevations of the valley floor and the plain to be equal. In the case of the valley, the same energy is used to heat a smaller atmospheric volume than over the plain because the sloping valley sidewalls enclose less volume. The energy increment added to the valley atmosphere will thus result in a larger temperature change in the valley atmosphere than over the plain. Similarly, at night, when energy is lost through the equal horizontal areas at the tops of the volumes, the loss of energy is applied to a smaller volume within the valley, so that the valley atmosphere cools more strongly.

This concept, first proposed by Wagner (1932b), reinvestigated by Neininger (1982), and recently extended by Steinacker (1984) to account for realistic topography, can be quantified by defining a *topographic amplification factor* (TAF),

$$\tau = \frac{\left[\dfrac{A_{xy}(h)}{V_{\text{valley}}}\right]}{\left[\dfrac{A_{xy}(h)}{V_{\text{plain}}}\right]} \tag{2.2}$$

where $A_{xy}(h)$ is the horizontal area through which energy enters the tops of the volumes at height $z = h$, where h is the height above the valley floor or plain. For an actual valley, a planimeter can be used with a topographic map to determine $A_{xy}(h)$ and the relationship between $A_{xy}(z)$ and z, from which the underlying valley volume can be estimated. Here V_{plain} is simply the product $hA_{xy}(h)$. This form of the TAF definition emphasizes volumetric comparisons between a valley and the adjacent plain. Yet an-

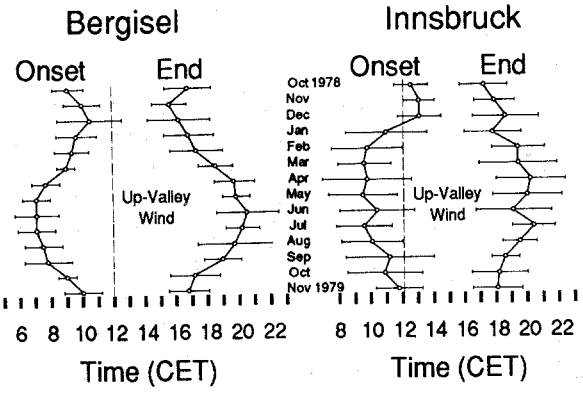

FIG. 2.5. Onset and cessation times for the down-valley wind at Innsbruck, Austria, and on a 200 m hill (Berg Isel) on the valley floor near Innsbruck as a function of month of year. Standard deviations are given as horizontal lines. (Dreiseitl et al. 1980.)

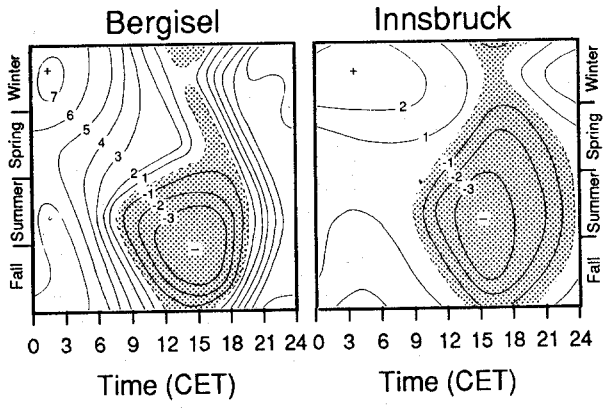

FIG. 2.6. Daily and yearly course of the along-valley wind speed components at Berg Isel and Innsbruck. Negative wind speeds are up-valley components. (Dreiseitl et al. 1980.)

TABLE 2.6. Number of valley wind days in the Inn Valley as a function of weather type, and the annual frequency of valley wind days (Vergeiner 1983).

Location	N, NE, E	SE, S, SW	W	NW	H	V	Total (year)
Kufstein	22	38	11	15	51	27	32%
Berg Isel	27	20	32	33	65	36	40%
Meteor. Inst.	24	15	24	22	43	28	29%
Zenzenhof	41	35	56	45	77	46	53%

Cardinal directions indicate direction of upper winds.
H = high pressure and weak gradients aloft.
V = variable upper winds.

other form of the TAF definition can be used to calculate topographic amplification factors for valley cross-sections. In that case, for a simple, unit-thickness, vertical valley cross-section, the TAF can be defined as

$$\tau = \frac{\left[\frac{W}{A_{yz_{\text{valley}}}}\right]}{\left[\frac{W}{A_{yz_{\text{plain}}}}\right]} \qquad (2.3)$$

where W is the width at the top of the two cross sections and A_{yz} is the area of the vertical cross-section. This formula is used to illustrate the calculation of τ for several idealized valley cross-sections of depth D, as shown in Fig. 2.9a. In the top part of the figure are cross sections for U- and V-shaped valleys, as well as for a valley with convex sidewalls. For illustration, the figure is drawn for valleys that are twice as wide as they are deep. The lower part of the figure shows cross sections for valleys with similar sidewall shapes, but with a horizontal valley floor of width L. The denominator of (2.3), the area to volume ratio for the plain, is simply $1/D$. Evaluation of (2.3) for the plain, and for the U-shaped, V-shaped, and convex valleys results in topographic amplification factors of 1, 1.27, 2, and 4.66, respectively, for the cross sections. For valley cross-sections with the same sidewall shapes, but with wider valley floors (Fig. 2.9b), the topographic amplification factors are reduced, approaching unity as the valley floor widens. Clearly, the valley with convex sidewalls, having less volume for the same area at its top, will have a substantially larger diurnal temperature range, if the energy change is confined within the volume. We tend to think of valleys as V-shaped or U-shaped because we typically view valleys from their floors, but valley drainage

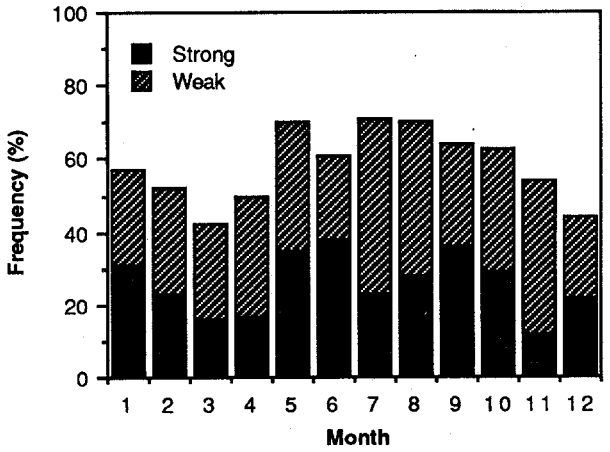

FIG. 2.8. Frequency of weak and strong drainage flows in Colorado's Brush Creek valley as a function of month of year. (Adapted from Gudiksen 1989.)

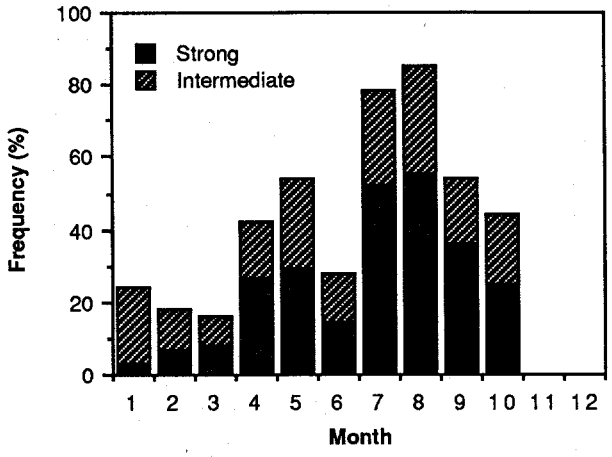

FIG. 2.7. Frequency of weak and strong drainage flows in California's Anderson Creek valley as a function of month of year. (Adapted from Gudiksen and Walton 1981.)

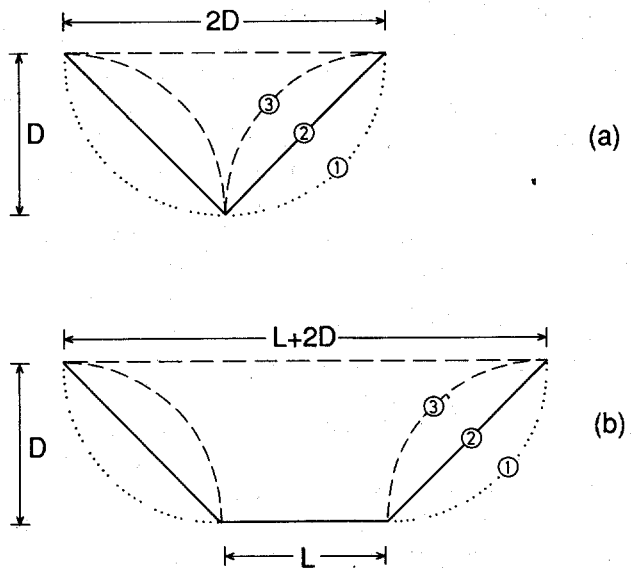

FIG. 2.9. Calculation of topographic amplification factors for idealized valleys of various cross sectional shape with (a) no horizontal valley floor, and (b) horizontal valley floor. (Müller and Whiteman 1988.)

areas typically have a pronounced convex shape in their upper sections.

According to Steinacker (1984), Wagner (1932b) originally made TAF calculations of diurnal temperature ranges and horizontal pressure gradients for a U-shaped section of the Inn Valley. These calculations gave horizontal pressure gradients that were somewhat smaller than observed. Subsequent calculations by Steinacker, including the Inn Valley and its tributaries, showed a substantially larger TAF, because of the preponderance of convex sidewalls in the tributaries and upper levels of the main valley. Steinacker's calculations have spawned a number of calculations by others, and reassessments of previous work, such as that of Whiteman and McKee (1982), in which calculations of TAFs were originally done using geometrically idealized cross sections. Böhm (1985) incorporated Steinacker's method in a version of the Whiteman and McKee inversion destruction model for Swiss topography. Müller and Whiteman (1988) used Steinacker's method of calculating TAFs to simulate the breakup of a valley temperature inversion in Switzerland's Dischma Valley. A key aspect of Steinacker's work that has received less attention is the effect of stability on the development of horizontal pressure gradients. According to Steinacker, stability may be effective in confining energy input to certain altitudes in the valley. If the energy is confined to the upper levels of a valley where large atmospheric volumes are present, the temperature change at that level will be small. On the other hand, if energy input is confined to lower altitudes in the valley where atmospheric volumes are small, temperature changes will be large. Through the hydrostatic equation, pressure depends on the mass of the column of air above the point of interest which, in turn, depends on the temperature distribution in the column. Small temperature changes at the upper altitudes of the valley will have less effect on the vertical pressure distribution than large temperature changes at the lower altitudes, even though the same amounts of total energy input may be involved in producing the respective temperature changes.

McKee and O'Neal (1989) carried Steinacker's approach a step further. Rather than considering that the valley-plain pressure gradient drives the valley winds, they postulated that valley winds can be driven by along-valley pressure gradients that develop within a valley due to variations of valley geometry along the valley's length. One can investigate the effect of the topography in developing such gradients by making TAF calculations with (2.3) at a number of points along a valley's axis, as calculated in Table 2.5 for Austria's Inn Valley. Stronger nighttime cooling at the head of a valley than at its mouth would result in a pressure gradient that would drive down-valley circulations. Calculations of TAF ratios along a valley's axis would allow one to determine whether the valley has a vigorous along-valley circulation or whether cold air would stagnate and pool in one or more segments of a valley. McKee and O'Neal made such calculations for several valleys in Colorado where wind data were available, and verified that the geometric calculations agreed with existing wind data (Fig. 2.10). This initial success has implications for future dynamic modeling of valley wind systems; it suggests that the TAF concept may be used to compare the model terrain to the actual terrain to verify that thermodynamic effects in the modeled terrain are realistic relative to the actual terrain being modeled.

The topographic amplification factor is purely a geometrical factor describing the valley topography. The influence of this factor on the valley's thermal structure and wind systems may be strengthened or weakened by other

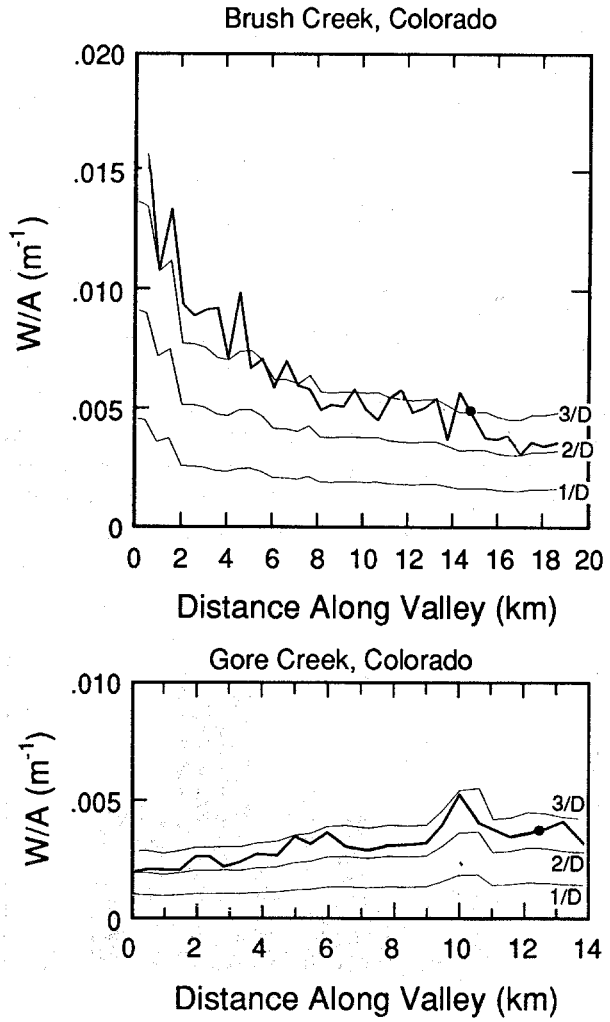

FIG. 2.10. Width to cross sectional area ratios for a draining valley (Brush Creek valley) and a pooling valley (Gore Creek valley). In the draining valley the width to area ratio decreases with down-valley distance; in the pooling valley the ratio increases. (McKee and O'Neal 1989.)

processes. First, since energy gain and loss from the valley volume occur primarily at the valley surfaces (i.e., valley floor and sidewalls), an efficient means of transport of energy from the sidewalls to the entire valley volume is required in order to drive the along-valley wind system. The valley volume is enclosed by topography so that radiation, conduction, and convection from the surfaces are relatively more effective in transporting energy than would be the case over a flat plain. The upslope and downslope flows, as we will see shortly, are especially adept at efficiently transporting energy to and from the entire valley volume. Second, if the energy gains and losses are to be effective in driving local wind systems in the valley, the energy gains and losses must be confined to the valley, rather than dissipated into the air above the valley. Observations show that one of the effects of valley geometry, at least under weak-to-moderate gradient wind conditions, is to limit the dynamic exchange between the air above the valley and the air within the valley (e.g., see Maki and Harimaya 1988). Finally, the effect of the geometrical factor can be strengthened or weakened by plain-valley or along-valley gradients of energy gain or loss. For example, gradients in albedo or soil moisture along a valley's axis may produce along-valley sensible heat flux gradients that may modify the topographically developed differences in diurnal temperature range between valley and plain or along a valley's axis.

The TAF concept provides an explanation for strong along-valley wind systems that develop in valleys like the Inn Valley having a weak valley floor slope ($\approx$0.001 between Innsbruck and the Alpine foreland). Following this concept, a valley cut into a mountain range surrounded by a plain and having an absolutely horizontal valley floor (Fig. 2.11) could still have a strong valley wind system because the topographic amplification factor produces a greater diurnal temperature range in the valley atmosphere than above the surrounding plain.

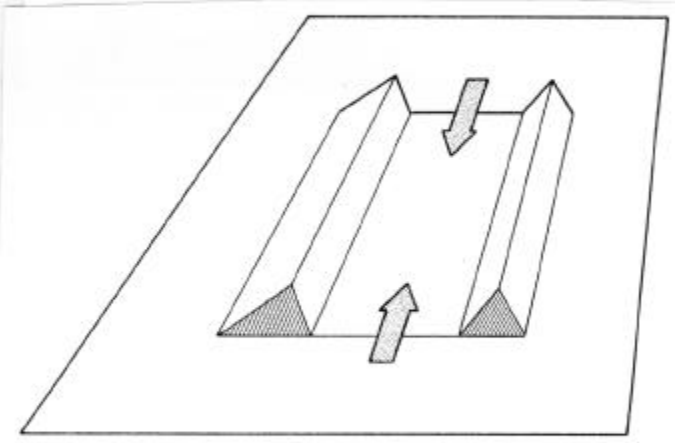

FIG. 2.11. A valley with a horizontal valley floor will still generate along-valley wind systems because the topographic amplification factor will produce a higher daily temperature range in the valley than over the surrounding plain.

2.2.2.2. EQUATIONS FOR THE VALLEY WIND SYSTEM

The following simplified set of equations can be used to illustrate the development of an along-valley wind system, the key physical processes involved, and the relationships between conservation equations:

$$\frac{\partial\theta}{\partial t} + u\frac{\partial\theta}{\partial x} + v\frac{\partial\theta}{\partial y} + w\frac{\partial\theta}{\partial z} = -\frac{\partial}{\partial x}(\overline{u'\theta'}) - \frac{\partial}{\partial y}(\overline{v'\theta'}) - \frac{\partial}{\partial z}(\overline{w'\theta'}) + \frac{\partial Q^*}{\partial z} \quad (2.4)$$

$$\frac{\partial u}{\partial t} + u\frac{\partial u}{\partial x} + v\frac{\partial u}{\partial y} + w\frac{\partial u}{\partial z} = -\alpha\frac{\partial p}{\partial x} + F \quad (2.5)$$

$$\frac{dp}{p} = -\frac{gdz}{RT} \quad (2.6)$$

$$\frac{\partial u}{\partial x} + \frac{\partial v}{\partial y} + \frac{\partial w}{\partial z} = 0 \quad (2.7)$$

$$p\alpha = RT, \quad (2.8)$$

where θ is potential temperature, u, v, and w are velocity components in orthogonal directions x, y, and z, t is time, Q^* is net all-wave radiation flux, α is specific volume, p is pressure, F is friction, g is gravitational acceleration, R is the gas constant, and T is temperature. The dependent variables have been averaged over some appropriate time scale, and overbars have been dropped except for the Reynolds terms. Two temperature variables have been used in the equations to facilitate discussions to follow. The defining equation for potential temperature is

$$\theta = T\left(\frac{1000}{p}\right)^{\frac{R}{c_p}}, \quad (2.9)$$

where the units of p are hectopascals. The equations, in order, are the thermodynamic energy equation, the x-momentum equation, the hydrostatic equation, the mass continuity equation, and the equation of state.

A somewhat heuristic or simplified view of the development of the along-valley circulation comes from considering (2.4) through (2.8) in turn for two unit vertical cross-sections in a valley at different down-valley distances. The atmosphere is initially considered stationary.

Different heating rates may be produced in the two cross sections by sensible and radiative flux convergence following (2.4). The amount of heating produced in the cross section depends on the topographic amplification factor, as we have described. Integrating (2.6) downward from a common pressure surface, we can calculate the pressure distribution in the column as a function of height. The cooler column will have a higher pressure at each height, so that an along-valley pressure gradient will be developed [$\partial p/\partial x$ in Eq. (2.5)], producing an acceleration that generates an along-valley wind. This acceleration is opposed by friction. Motions are constrained to occur so that, following (2.7), atmospheric mass is conserved. Once motion is initiated, advective terms become important in the thermodynamic energy and momentum equations. These terms do not generate cooling or momentum, but act to redistribute these quantities.

2.2.3. *Radiation and surface energy budgets*

A full understanding of the mechanisms by which heat is transferred to and from the valley atmosphere to generate along-valley flows requires an investigation of the budgets of mass, heat, and momentum for valley volumes using conservation equations (2.4), (2.5), and (2.7). Present experimental efforts along these lines are discussed in section 2.2.4. First, however, it will be convenient to review what is known concerning the radiation and energy budgets of the valley surfaces, since these constitute the lower boundary condition for the atmospheric volume, and it is largely through this lower surface that the valley atmosphere is warmed and cooled. Thus, we begin with a review of radiation and energy budget fundamentals at surfaces, illustrating the concepts with recent observational data from valleys.

Net all-wave radiation Q^* is the sum of net shortwave (K^*) and net longwave (L^*) radiation, such that

$$Q^* = K^* + L^*, \tag{2.10}$$

where net shortwave and longwave radiation are given as the sums of the appropriate incoming and outgoing radiation streams (Fig. 2.12a),

$$K^* = K\downarrow + K\uparrow, \tag{2.11}$$

$$L^* = L\downarrow + L\uparrow \tag{2.12}$$

and incoming shortwave radiation can be written as the sum of the direct (S) and diffuse (D) shortwave radiative components

$$K\downarrow = S + D. \tag{2.13}$$

The sign convention to be used here is that downward-directed radiation is positive and upward-directed radiation is negative. By combining (2.10) through (2.13) we can express the radiation budget as

$$Q^* = S + D + K\uparrow + L\downarrow + L\uparrow. \tag{2.14}$$

This expression allows one to calculate net all-wave radiation at a surface at a given instant in time. Measurements on clear days show that, typically, net all-wave radiation is a large positive value during the day and a small negative value during the night. This points out the general lack of a radiative balance at a given instant in time, or diurnally. Deficits or excesses in the radiation budget must be made up through fluxes of energy from nonradiative sources (Fig. 2.12b), following the expression for the energy balance of a surface:

$$Q^* + Q_G + Q_H + Q_E = 0, \tag{2.15}$$

where Q^* is net all-wave radiation, Q_G is ground heat

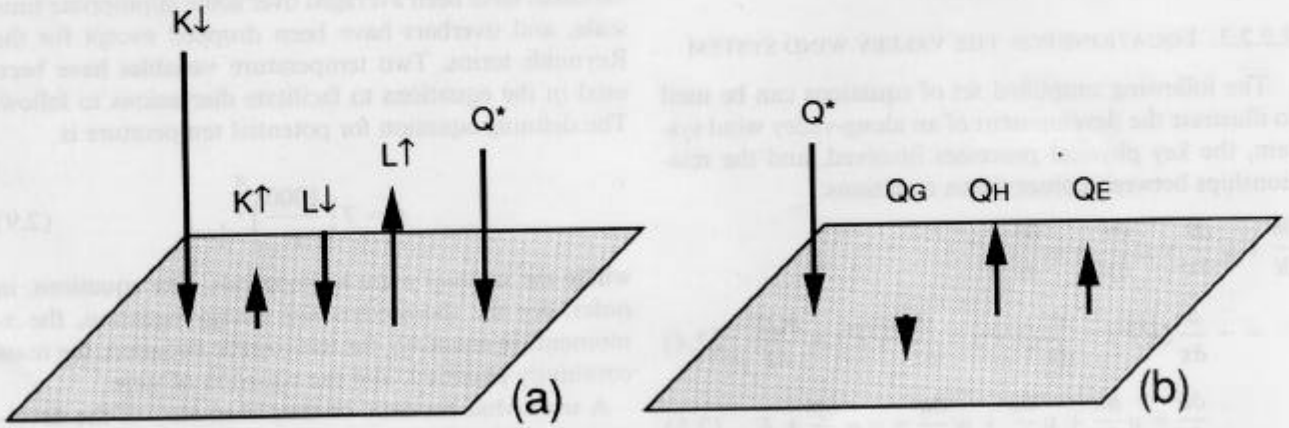

FIG. 2.12. Components of (a) the radiation budget, and (b) the surface energy budget on a horizontal surface. Here $K\downarrow$ = incoming solar radiation, $K\uparrow$ = reflected solar radiation, $L\downarrow$ = incoming longwave radiation, $L\uparrow$ = outgoing longwave radiation, Q^* = net all-wave radiation, Q_G = ground heat flux, Q_H = sensible heat flux, and Q_E = latent heat flux. The components shown are scaled to represent midday values of the radiation and surface energy budgets for a dry continental valley in the fall.

flux, Q_H is surface sensible heat flux (over flat terrain usually considered to be given by the single term $\rho c_p \overline{w'\theta'}$), and Q_E is latent heat flux. In this equation we use the convention that all fluxes toward the surface, whether from the atmosphere or the ground, are considered positive.

Following this expression, excess radiative energy (e.g., during daytime) may be used to heat the ground, warm the atmosphere, or evaporate water. Radiative energy deficits during nighttime may be balanced by an upward flux of heat from the ground, a downward flux of heat from the atmosphere, or condensation of water on the surface. Note that (2.15) states only that the sum of the terms is zero; it gives no information on how a change in one term will be partitioned into the other terms. Such partitioning may involve differing signs among the three remaining terms.

Thermally developed valley wind systems are driven by heat transfer to and from the valley atmosphere, so that our primary interest in the radiation and surface heat budgets is the estimation of sensible heat flux. Direct measurements of sensible (and latent) heat flux are notoriously difficult to make on heterogeneous sloping surfaces. Estimation of sensible heat flux often involves measurement of the individual terms in (2.15), under the overall constraint that the surface energy budget must be balanced. Ground heat flux measurements are also problematical in complex terrain, although, like sensible and latent heat fluxes, several different measurement methods are available (Kimball et al. 1976). Definitive net radiation measurements are largely unavailable for mountains of the western United States, even though rather extensive measurements of solar, thermal, and net radiation were reported in the Alps in the 1950s (Sauberer and Dirmhirm 1958), and the required equipment is simple and reliable. If the measurements of individual terms in (2.15) were straightforward and error-free, there would still be the question of the representativeness of the point measurements for estimating sensible heat flux over the valley as a whole. An initial approach to estimating variability of energy budget terms in complex terrain has been to consider that the surface energy budget is driven primarily by net radiative gains during daytime and losses during nighttime, and to estimate the spatial variability of such gains and losses by investigating the contributions to net radiation from individual terms in the radiative energy budget (2.14). In the next section an initial step in this approach is illustrated for Colorado's Brush Creek valley.

2.2.3.1. Radiation Budget

As part of the 1984 ASCOT experiment (Table 2.3), radiation budget component measurements were made at five sites in Colorado's 650-m-deep Brush Creek valley. (See Fig. 2.13 for the site locations and a topographic map of the experimental area.) In the dry, high-altitude, Brush Creek valley, observations (Whiteman et al. 1989a,b) showed a large direct-beam solar radiation component in the radiation budget, so that slope aspect and inclination angles of the valley surfaces had a strong effect on incoming solar radiation. Surface properties, including vegetation cover and soil moisture, were important in explaining differences in reflected radiation and outgoing longwave radiation between sites. These differences were especially significant between the dry, barren, southwest-facing sidewall and the opposing, relatively moist, brushy, northeast-facing sidewall. Daily totals of radiation and surface energy budget parameters varied significantly between sites depending on the length of the daytime period, and thus on local sunrise and sunset times at individual stations. Large daytime net radiation gains and nighttime losses were experienced on the mesa-shaped ridgetop of the valley, supporting the concept of the ridgetops being elevated heating surfaces during daytime and cooling surfaces during nighttime. Observations averaged over a 15-day period of variable weather illustrated the general effect

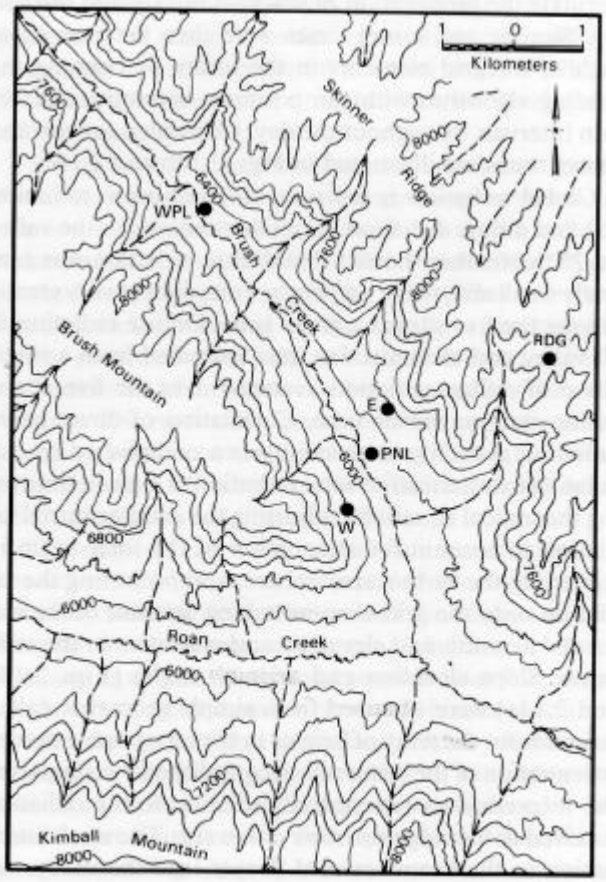

FIG. 2.13. Locations of radiation and surface energy budget measurement stations in the Brush Creek valley, September–October 1984.

of cloudy weather in reducing contrasts in radiation climate among sites.

The spatial variations in climatic contrasts experienced within this dry, high-elevation, continental valley can be illustrated with the help of a digital terrain model. The reader interested in reviewing recent progress in the modeling of solar and longwave radiation fields in complicated terrain areas is referred to prior work by Marks and Dozier (1979), Dozier (1980), Isard (1983), and Olyphant (1984, 1986a,b). For the Brush Creek valley, modeled spatial patterns of global radiation on 25 September 1984 will be used to illustrate variations in instantaneous and daily total surface microclimates. The date in question is near the autumnal equinox when the sun rises due east and sets due west with a 12-h daylight period.

A digital terrain model of the Brush Creek valley region was produced using a 30-m grid interval. A small subdomain was chosen for modeling, representing a segment of the Brush Creek valley running up-valley from the Brush–Roan Valley confluence for 8 km and bounded by the valley ridgetops (Fig. 2.14a). Using this model, combined with theoretical equations for the sun's movement through the sky on the date of interest (Whiteman and Allwine 1986), a solar shading algorithm was used to simulate the propagation of shadows throughout the valley. Sunrise and sunset times were then determined at each of the grid elements in the valley by running the shading algorithm with sun positions determined at 10-min intervals throughout the day. Calculated sunrise and sunset times are illustrated in Figs. 2.14b and 2.14c.

Global radiation is the sum of direct-beam radiation (S) and diffuse radiation (D). Observations in the valley on 25 September showed that diffuse radiation was generally small and, while varying in time, did not vary greatly among the five sites at a given time. Diffuse radiation at all valley grid elements was thus estimated from a single curve of diffuse radiation averaged over the five observation stations versus time. Calculation of direct beam radiation at each grid element was accomplished by calculating extraterrestrial solar radiation at a given time using theoretical equations, adjusting the extraterrestrial radiation to account for attenuation of the solar beam in traversing the earth's atmosphere, and projecting the radiation onto the grid element taking account of the elements' azimuth and elevation angles relative to the solar beam. Slope elevation and azimuth angles (Figs. 2.14d and 2.14e) were obtained from simple geometric calculations from the array of heights in the topographic model. Attenuation of the beam was accomplished by comparing the theoretical extraterrestrial radiation to the radiation received at the ridgetop observation site. The weak attenuation as the beam traveled deeper into the valley was determined by developing an empirical attenuation versus altitude relationship from measurements at the five sites.

The resulting calculations of global radiation are shown in Fig. 2.14f for 0730 MST 25 September. At this time, the east sidewall was in shadow and the maximum global radiation was received on steeply inclined east-facing surfaces on the west sidewall. Since all surfaces receive diffuse radiation, the global radiation was positive even on the shaded east sidewall. At 1600 MST (Fig. 2.14g) the west sidewall was in shadow and strong insolation was received on the east sidewall. Strong contrasts in insolation were present between the east and west sidewalls, as expected, but strong contrasts were also present between adjacent terrain elements on the east sidewall on account of shadows and differences in aspect and inclination angles. By integrating such instantaneous global radiation fields generated at 10-min intervals through the course of a day, a daily total global radiation field was determined, as shown in Fig. 2.14h. Daily totals varied over an order of magnitude at different locations in the valley. Ridgetop sites were favored by the long period of direct beam radiation relative to shaded locations deeper in the valley. Inclined south- and southwest-facing slopes received daily totals exceeding 26 MJ m^{-2}, while north-facing slopes in box canyon tributaries of the west sidewall received daily totals less than 3 MJ m^{-2}. Daily totals were generally much higher on the valley's east sidewall than on the opposing sidewall, but interesting differences occurred within the finestructure of the topography on each sidewall. Thus, the field of daily total global radiation on the west sidewall contains a mosaic of microclimatic regimes, with pronounced differences occurring over very small spatial scales.

The amount of incoming longwave and diffuse radiation received on a surface in complex terrain depends on the fraction of the sky visible in the viewing hemisphere of the surface, called the sky view factor. For a simple valley cross-section with a horizontal valley floor and two linear sidewalls of different inclination angles the smallest sky view factors on the slopes will occur at their bases (Petkovsek 1978c). On the valley floor, view factors will increase as the valley center is approached. Figure 2.15 provides an example of sky view factor calculations for Colorado's Brush Creek valley, computed from a 30-m resolution digital topographic model using the formula

$$\beta = \frac{1}{n} \sum_{i=1}^{n} (1 - \sin\phi(\theta_i)) \qquad (2.16)$$

where $n = 2\pi/\Delta\theta$, $\Delta\theta = 10°$ is the azimuth angle increment, and $\phi(\theta_i)$ is the mean elevation angle of the horizon over the azimuth angle increment $\Delta\theta$ centered around azimuth angle $\theta_i = (i - 0.5)\Delta\theta$. In the figure the lightest shade of gray represents a view factor of 1 and the darkest shade of gray represents the lowest calculated sky view factor of 0.47. The mesa tops on either side of the Brush

Creek valley have high sky view factors, but the view factors drop rapidly with depth in the valley. The smallest view factors are at the base of cliffs in the box canyons that feed Brush Creek along its length. The valley center has noticeably higher sky view factors than at the lower edges of the sidewalls.

The distribution of sky view factors in real valleys causes complicated spatial variations in the downward longwave and diffuse solar radiation components. Locations with high sky view factors are exposed to the cold radiating sky and receive relatively small downward longwave radiative fluxes. As one descends deeper and deeper into a valley the effect of the relatively warm radiating sidewalls (compared to the cold radiating sky) increases the downward longwave irradiance. Other things being equal, this results in a decrease in nighttime radiative loss with distance below the ridgetops. Given equivalent outgoing longwave, soil, and latent heat fluxes, downward sensible heat flux from the near-ground layer of air should be enhanced [Eq. (2.15)] by this sky view factor effect, with the result that the upper slopes and ridgetops should prove to be more effective generators of cold air at night than the lower slopes.

Actual calculation of the downward irradiance at a surface element in a valley must be accomplished with the radiative transfer equation, and will depend on the sky view factor, atmospheric profiles of radiatively active gases (water, carbon dioxide, ozone) and the distribution of radiating temperature on the sidewalls. McKee and Whiteman (1977) made such calculations for a circular basin with a flat valley floor of 1 km diameter and 31° sidewall slopes, for isothermal sidewalls at temperatures that varied from 20°C colder to 20°C warmer than the base of the temperature sounding. Calculations were performed using average summer and winter temperature and humidity soundings at Grand Junction, Colorado. At the valley floor center the decrease of net radiative loss from values calculated over a flat plain having the same atmospheric profiles can vary from 8% to 24% depending on the radiating temperature of the sidewall. The largest relative decreases occur for dry winter soundings.

2.2.3.2. Surface Energy Budget

Few observations of sensible heat flux are yet available in valleys because of difficulties inherent in making the measurements. Several sets of measurements are now available, however, to illustrate the essential differences between levels of sensible heat flux in different climate settings.

Observations on the floor of Switzerland's Dischma Valley (Fig. 2.16) on the clear day of 6 August 1980 show that, in daytime, much of the available energy is used for evapotranspiration (Halbsguth et al. 1984). Sensible heat flux, while somewhat larger than ground heat flux, is only about 40% of the latent heat flux. Observations on this day followed a period of heavy rain, suggesting that the results may not be entirely typical. On the clear day of 7 September 1980 on the floor of Austria's Inn Valley (Fig. 2.17), daytime net radiation was much weaker than experienced a month earlier in the Dischma Valley. Only a small fraction of the net radiation was used to heat the ground, and most of the available energy was used for evapotranspiration. Sensible heat flux was about a third of the daytime integrated latent heat flux (Vergeiner and Dreiseitl 1987).

A comparison can be made between the more moist Alpine setting and Colorado's semiarid Brush Creek valley. Brush Creek valley observations (Fig. 2.13) were made at 5 sites—two on the valley floor (PNL and WPL sites), one on the ridgetop above the valley (RDG), and one on each of the opposing valley sidewalls (E and W). The Brush Creek dataset (Fig. 2.18) is characterized by large values of net radiation for the date in question (7 weeks later in the year than the Dischma Valley data) and conversion of a high fraction of the available energy into sensible heat flux. Peak sensible heat flux values at some of the sites are larger than the net radiation peak in the Inn Valley. The Colorado valley is thus characterized by very high rates of energy transfer to the overlying valley atmosphere during daytime (Whiteman et al. 1989b)—a feature of the climate that strongly affects the development of local wind systems.

Strong contrasts in instantaneous latent and sensible heat fluxes occurred between the opposing northeast- and southwest-facing sidewalls of the Brush Creek valley as solar insolation varied through the course of the day and as shadows propagated across the valley. This differential heating and moistening of the air above the opposing slopes produced cross-valley circulations that resulted in redistribution of moisture and heat throughout the valley volume. The cross-valley circulations strongly affected the morning breakup of artificial tracer plumes introduced into the valley (Whiteman 1989; Bader and Whiteman 1989; Gudiksen and Shearer 1989).

The ridgetop site, with a nearly unobstructed view of the sky and the longest daytime period, received the highest daily total of net radiation and the highest sensible heat flux total. The dry southwest-facing slope produced a nearly equivalent daily total sensible heat flux, despite the later sunrise and earlier sunset at this site, because of the dry soil, lack of vegetation, and intense afternoon radiation on the sloping surface. One of the valley floor sites, located in a wheatgrass meadow, produced a daily total latent heat flux over four times larger than the dry southwest-facing sidewall. Mean daytime Bowen ratios (sensible/latent heat flux ratio) varied from 0.86 at the valley floor meadow site to 7.60 on the southwest-facing

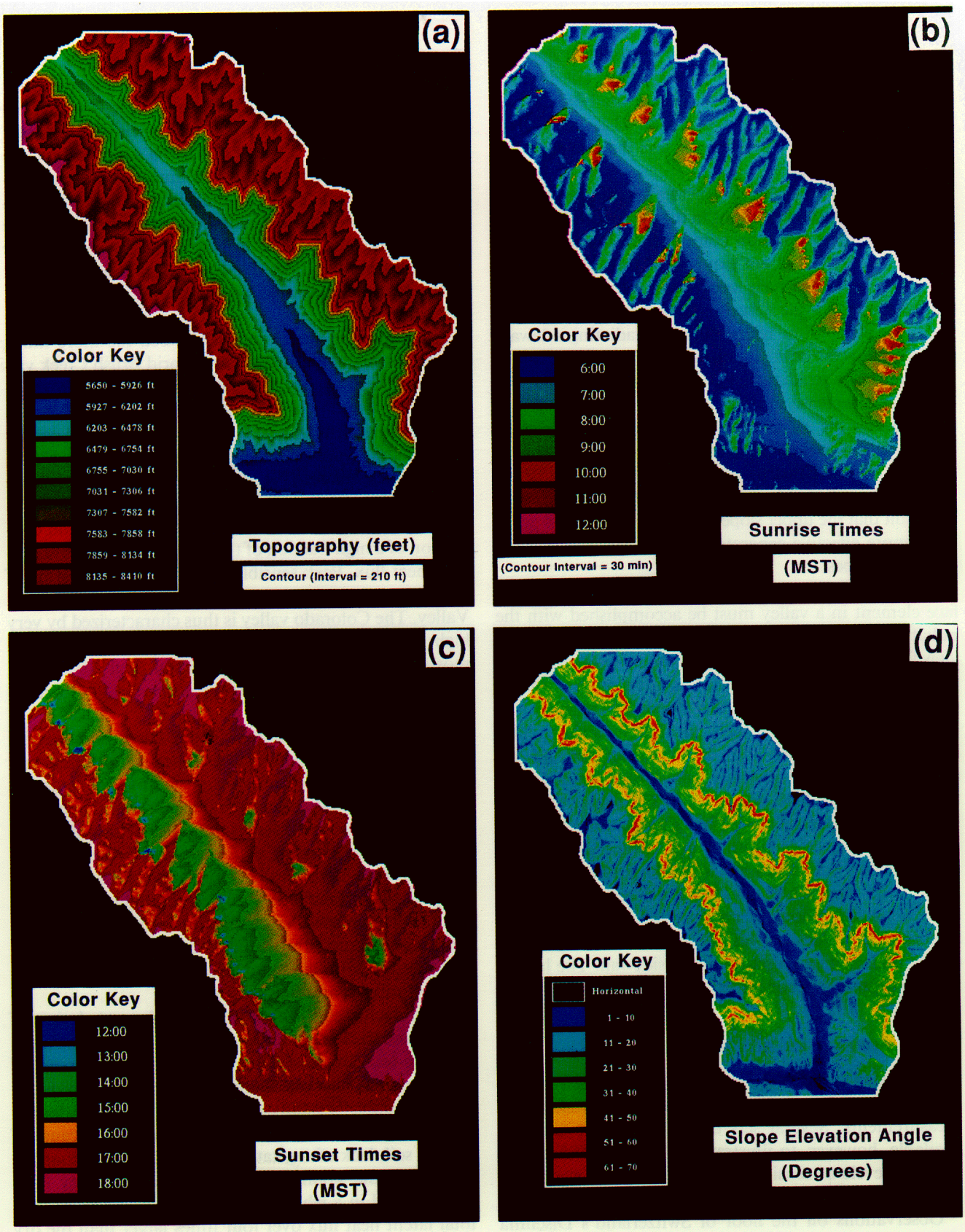

FIG. 2.14. Illustration of topographic and microclimatic variations in Colorado's Brush Creek valley on 25 September 1984. (a) Topography, (b) sunrise time, (c) sunset time, (d) slope elevation angle.

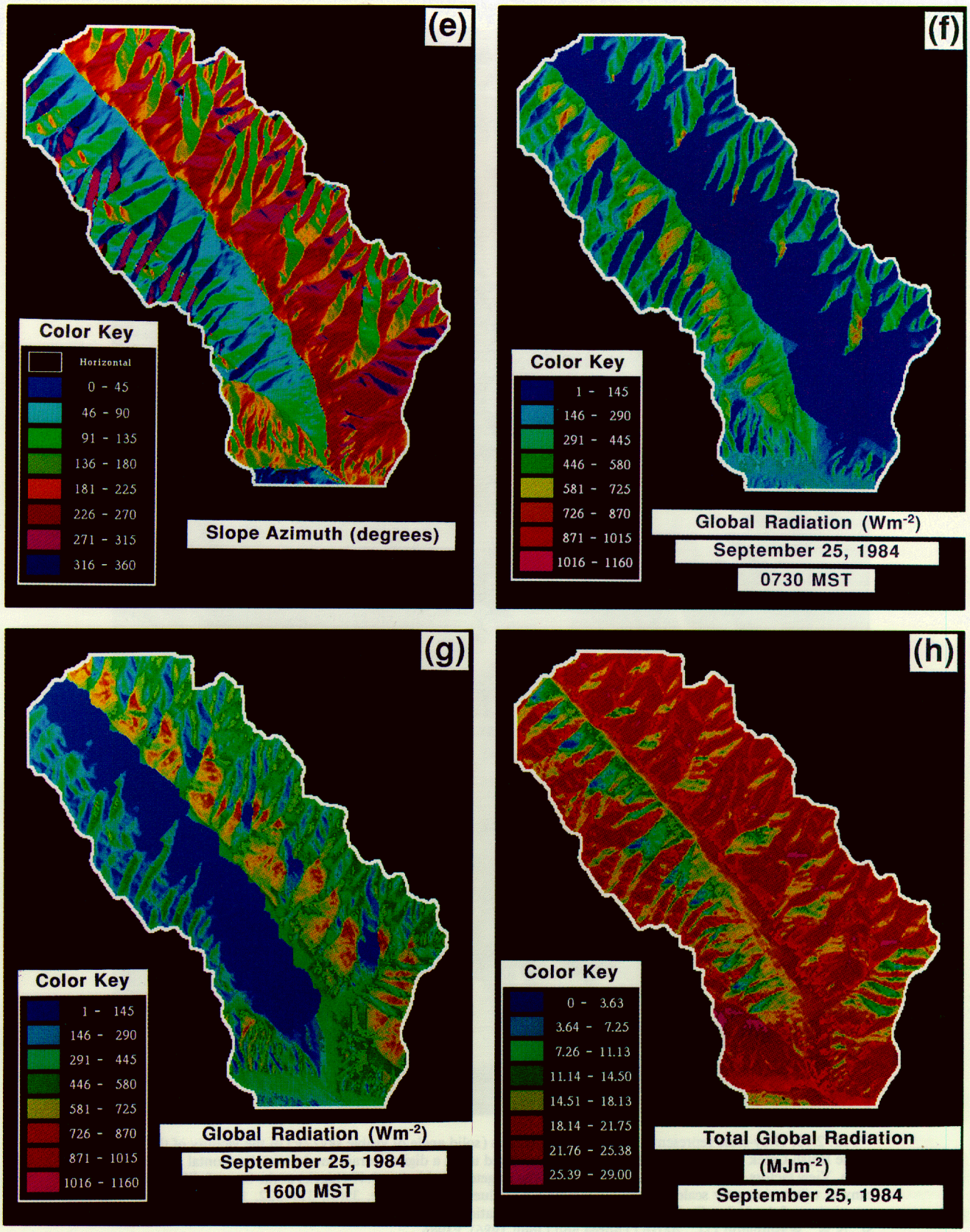

FIG. 2.14, continued. (e) slope azimuth angle, (f) global radiation at 0730 MST, (g) global radiation at 1600 MST, (h) daily total global radiation.

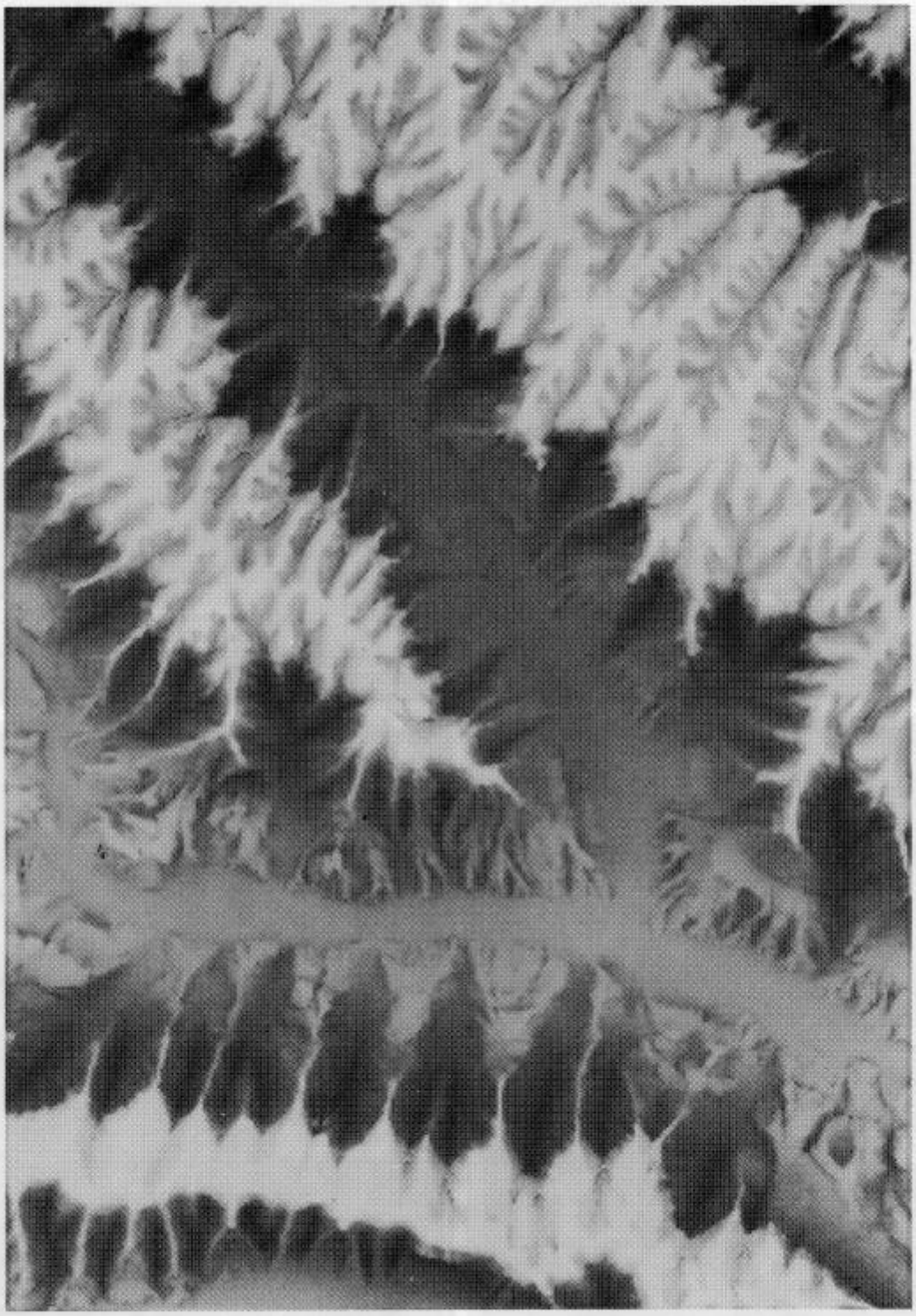

FIG. 2.15. Gray-scale representation of sky view factors (solid angle of visible sky/2π) in the vicinity of the mouth of the Brush Creek valley. Sky view factors were calculated using a digital terrain model with horizontal resolution of 30 m. View factors in the scene range from 1.00 at the ridgetops (white) to 0.47 (black) at the base of cliffs within box canyon tributaries; gray scales represent intermediate values (*Weatherwise*, 39(6), 319–322, 1986.) Reprinted with permission of the Helen Dwight Reid educational foundation. Published by Heldreff Publications, 4000 Albemarle St., N.W., Washington D.C. 20016 (Thorpe and Orgill 1986). ©1986.

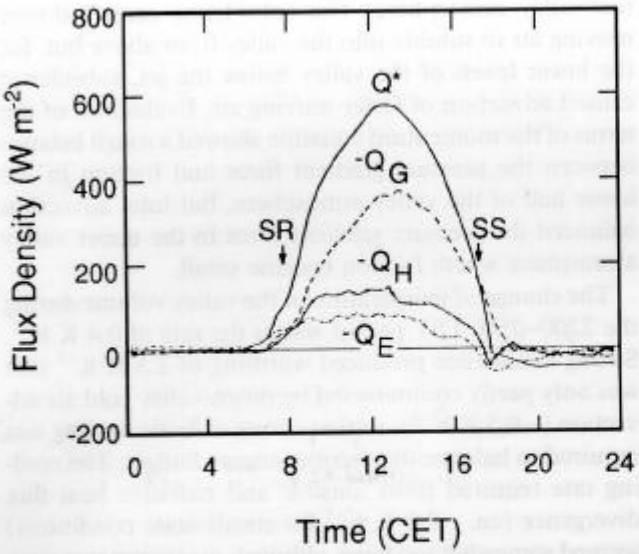

FIG. 2.16. Surface energy budget for the Dürrboden site in Switzerland's Dischma Valley during the DISKUS experiment, 6 August 1980. (Halbsguth et al. 1984.)

sidewall. Thus, we see that significant spatial differences in instantaneous and daily total sensible heat fluxes occur within complex terrain areas.

Daily total sensible heat fluxes in the valley as a whole were much larger than required to destroy typical nocturnal temperature inversions, and the excess was available on clear fall days to grow deep convective boundary layers over the region. The times of reversal of the slope wind systems at the individual energy budget sites were closely related to the time of sign reversal of sensible heat flux.

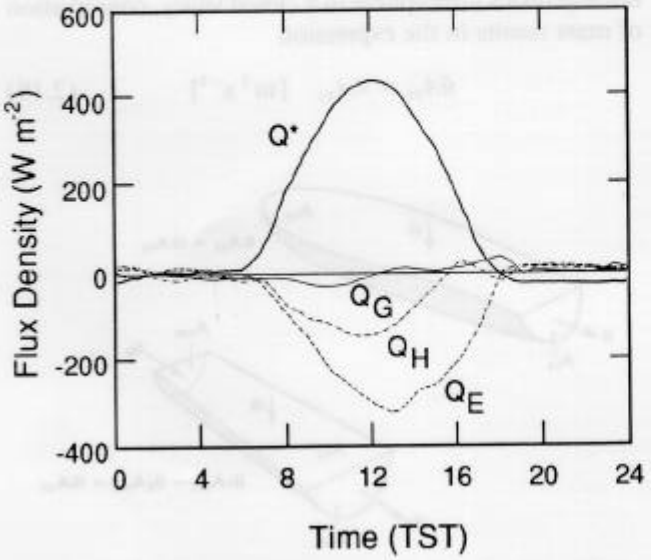

FIG. 2.17. Radiation and surface energy budgets for a site on the floor of the Inn Valley, 7 September 1980. (Vergeiner and Dreiseitl 1987.)

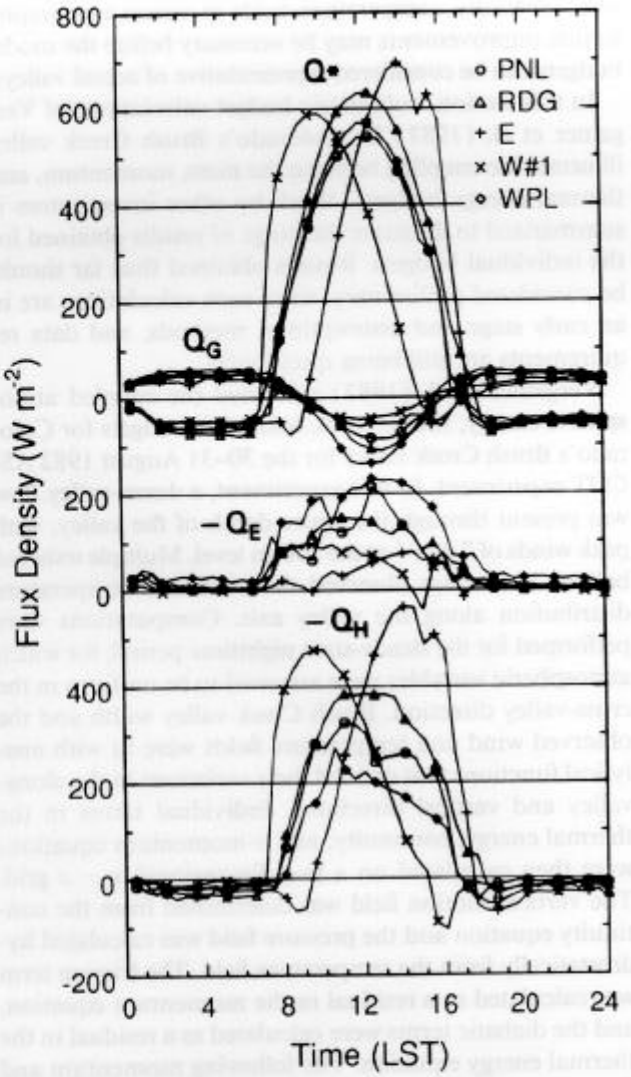

FIG. 2.18. Surface energy budgets at five sites in the Brush Creek valley, Colorado, during the ASCOT experiment, 25 September 1984. (Whiteman et al. 1988b.)

Thus, the evolution of the wind systems at individual sites is strongly dependent on sensible heat input into individual topographic elements within the valley.

2.2.4. *Atmospheric budgets of mass, heat, momentum, and moisture*

Several recent major field studies have investigated atmospheric budgets of mass, heat, momentum, and moisture in valley circulations. Initial studies have generally investigated individual budgets, although in actual atmospheric flows all budgets are inextricably coupled and must be simultaneously balanced. The initial observational studies are stimulating efforts to make such budget calculations from dynamic models. Present models have not been entirely successful in simulating realistic wind

and, especially, temperature fields in actual topography so that improvements may be necessary before the model budgets can be considered representative of actual valleys.

In this section, volumetric budget calculations of Vergeiner et al. (1987) for Colorado's Brush Creek valley illustrate the coupling between the mass, momentum, and thermal energy budgets. Work by other investigators is summarized to illustrate the range of results obtained for the individual budgets. Results obtained thus far should be considered preliminary, since such calculations are in an early stage and assumptions, methods, and data requirements are still being questioned.

Vergeiner et al. (1987) evaluated the coupled atmospheric energy, momentum, and mass budgets for Colorado's Brush Creek valley for the 30–31 August 1982 ASCOT experiment. In this experiment, a down-valley flow was present through the entire depth of the valley, with peak winds of 7 m s^{-1} at the 100-m level. Multiple tethered balloon soundings observed the wind and temperature distribution along the valley axis. Computations were performed for the steady-state nighttime period, for which atmospheric variables were assumed to be uniform in the cross-valley direction. Brush Creek valley width and the observed wind and temperature fields were fit with analytical functions that defined their variations in the along-valley and vertical directions. Individual terms in the thermal energy, continuity, and x-momentum equations were then calculated on a two-dimensional $x - z$ grid. The vertical motion field was determined from the continuity equation and the pressure field was calculated hydrostatically from the temperature field. The friction term was calculated as a residual in the momentum equation, and the diabatic terms were calculated as a residual in the thermal energy equation. The following momentum and thermodynamic energy equations illustrate the results obtained from these initial Brush Creek valley investigations. Under steady-state conditions, the terms have the signs indicated.

$$\frac{\partial u}{\partial t} = -u\frac{\partial u}{\partial x} - w\frac{\partial u}{\partial z} - \alpha\frac{\partial p}{\partial x} + \text{Friction}$$

$$0 = \quad + \quad \begin{matrix} -\,(\text{above jet}) \\ +\,(\text{below jet}) \end{matrix} \quad + \quad - \qquad (2.17)$$

$$\frac{\partial \theta}{\partial t} = -u\frac{\partial \theta}{\partial x} - w\frac{\partial \theta}{\partial z} + D$$

$$0 = \underbrace{\quad - \quad}_{} + \quad -$$

$$0 = \quad + \qquad -. \qquad (2.18)$$

The valley vertical motion field was found to be quite sensitive to small changes in the fit of the analytical function to the along-valley wind field. Along-valley mass flux divergence produced subsidence and warming throughout the valley atmosphere. The subsidence caused slower moving air to subside into the valley from above but, for the lower levels of the valley below the jet, subsidence caused advection of faster moving air. Evaluation of the terms of the momentum equation showed a rough balance between the pressure gradient force and friction in the lower half of the valley atmosphere, but total advection balanced the pressure gradient force in the upper valley atmosphere where friction became small.

The change of temperature of the valley volume during the 2200–0500 LST period was at the rate of 0.4 K h^{-1}. Strong subsidence produced warming of 2.5 K h^{-1} that was only partly counteracted by down-valley cold air advection (−0.5 K h^{-1}), so that strong diabatic cooling was required to balance the thermal energy budget. The cooling rate required from sensible and radiative heat flux divergence (ca. −2.0 K h^{-1} for steady-state conditions) seemed somewhat too large, although measurements were not available in the 1982 ASCOT experiment. The imbalance could have been caused by the horizontal homogeneity assumption used in calculating down-valley volume fluxes, which would cause subsidence warming to be overestimated. This assumption for the Brush Creek flow had been originally suggested by Whiteman and Barr (1986), but has since been shown to produce significant errors. This will be discussed further in section 2.2.4.1.

2.2.4.1. Conservation of Atmospheric Mass

Atmospheric mass conservation is often expressed in terms of volume fluxes rather than mass fluxes. The two fluxes are simply related by atmospheric density, which is near 1 kg m^{-3}. Mass conservation is illustrated for a closed valley and for a valley segment in Fig. 2.19. For a homogeneous atmosphere in a closed valley, conservation of mass results in the expression

$$\bar{u}A_{yz} = \bar{w}A_{xy} \quad [\text{m}^3\,\text{s}^{-1}] \qquad (2.19)$$

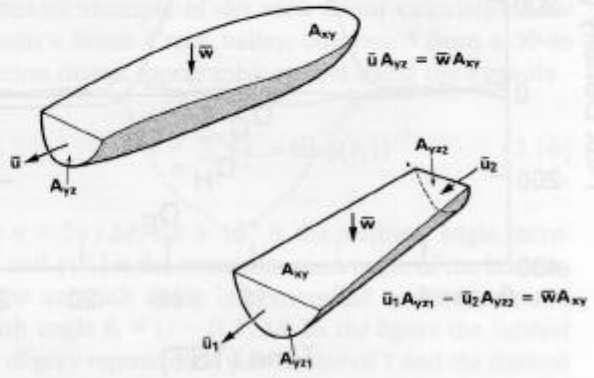

FIG. 2.19. Illustration of the mass budget for a closed valley (upper figure) and for a valley segment (lower figure).

where $\bar{u}$ is the mean along-valley wind speed averaged on a vertical $y - z$ plane and $\bar{w}$ is the mean vertical velocity averaged over the top of the valley atmosphere.

Most calculations of valley volume fluxes have been made for nighttime down-valley flows. The earliest such published calculations were apparently made by Ekhart (1944) for the Salzach Valley. Rao (1968, 1970) used such calculations to determine vertical motions from the mass continuity equation by assuming that measured mid-valley wind profiles were representative of winds on the entire cross section, from sidewall to sidewall. He found that mean down-valley wind speeds, as averaged over vertical cross-sections, increased with down-valley distance in three Vermont valleys during summer but, in the limit of long distances, tended to approach a constant value. Sinking motions at the top of the valley atmosphere on the order of several centimeters per second were required to balance the along-valley mass flux divergence. Whiteman and Barr (1986) made similar calculations for Colorado's well-drained Brush Creek valley in summer and found volume flux divergences that required subsidence rates of 15 cm s^{-1} or less in various segments of the valley. They stated that subsidence rates were, no doubt, overestimated by the horizontal homogeneity assumption. Since this work was published, lidar measurements in the Brush Creek valley (Post and Neff 1986) have provided new information on the cross-valley structure of the down-valley wind system. The horizontal homogeneity assumption in this narrow valley produces volume flux overestimates and mean vertical velocity overestimates of about 43% (Clements et al. 1989b; King 1989).

Calculations in Austria's Inn Valley, made by assuming that actual volume fluxes are 85% of those obtained with the horizontal homogeneity assumption, similarly show nocturnal along-valley volume flux divergence (Freytag 1987). Surprisingly, daytime measurements in the up-valley wind regime also show along-valley volume flux divergence. This suggests that net downward vertical velocities are the general rule in the segment of the Inn Valley investigated, except for possible rising motions that compensate the downslope flow during the brief evening transition. Freytag suggests that the daytime results, which were taken in a segment near the exit of the Inn Valley, may be a feature of the flow in that segment only, caused by a number of large tributaries just up-valley from the segment.

The presence of nighttime along-valley volume flux divergence requires compensatory subsidence over the valley. Such subsidence brings potentially warmer air into the valley during nighttime, warming the valley atmosphere. If the warming is too strong, the driving force for the along-valley circulation will disappear. Thus, the steady-state equilibrium is thought to be maintained by continuous diabatic cooling of the valley atmosphere. This cooling is facilitated by the topographic amplification factor, and the dynamic equilibrium is established through the combined action of the continuity equation, thermodynamic energy equation, and the momentum equation, involving friction at the valley floor and sidewalls.

The required net nocturnal subsidence is quite unlikely to occur uniformly over the valley cross-section since pre-cooled air would be thermodynamically preferred, and such air is available over the slopes and tributaries so that sinking rates may be enhanced there. During daytime, sinking motions over the valley center compensate the upslope flows to warm the valley atmosphere. During nighttime, however, the evidence is not clear. Are rising motions in the valley center required to compensate the downslope flows and produce cooling throughout the valley atmosphere, or do other terms in the thermodynamic energy equation (2.4) play a relatively more important role than the vertical advection term?

2.2.4.2. THERMAL ENERGY BUDGET

Atmospheric heat budgets have been computed in recent years for valley and basin atmospheres using data collected with motorgliders, tethered balloons, rawinsondes, Doppler sodars, and lidars. Most budgets have focused on the nighttime period when the wind and temperature structure change only slowly with time and the cooling is more or less confined to the valley; however, success at balancing such budgets has been mixed. The problem appears to be that the nighttime fluxes are relatively small, and measurement errors, particularly in the advective and sensible heat flux terms, can be relatively large.

Several conclusions can be derived from the nighttime thermal energy budget computations. In a well-drained valley, once the down-valley flow sets up and attains a reasonably steady state, the rate of cooling of the valley atmosphere becomes small. This is, no doubt, because air carried down the valley must be replaced by potentially warmer air from above. An approximate balance is apparently maintained between the inflow of this warmer air and the limited rate of cooling produced by the diabatic processes (sensible and radiative flux divergences). In closed basins, on the other hand, air can be cooled in place, with little warm air entrained from above, so that moderate rates of cooling can continue throughout the night. All studies to date have found radiative flux divergence to be small relative to sensible heat flux divergence. This conclusion, however, comes from model calculations of radiative flux divergence for plane parallel atmospheres, and does not properly account for within-valley processes such as radiation from the sidewalls. Advective terms are particularly important in well-drained valleys. The choice of coordinate system affects the calculated values of the individual advective terms so that it is necessary to look

at the sum of the advective terms to compare with other terms in the heat budget. Typically, the individual terms are large numbers of different sign and with significant errors, so that the sum is somewhat uncertain. Calculations suggest, however, that the advective sum is about the same size as the sensible heat flux divergence term. Thus, local closure of the heat budget within a small valley segment is not assured. Larger scale processes produced by the entire valley drainage area, including tributaries, affect the heat budget of a valley segment. This suggests that successful numerical modeling of the down-valley circulation system will require large three-dimensional model domains. Further, since important physical processes occur within the shallow downslope flows on the sidewalls, fine vertical grid resolution may be necessary.

We illustrate several key findings with reported heat budget computations. Heat budget studies have been published for Austria's Inn Valley (Freytag 1985), Switzerland's Dischma Valley (Hennemuth 1985), Colorado's Brush Creek valley (Horst et al. 1987), Japan's Akaigawa Basin (Maki et al. 1986), and Japan's Aizu Basin (Kondo et al. 1989). The Inn Valley is over 300 km long, 800 to 1500 m deep, and 10 km wide at the ridgetops. The valley structure is quite complicated, including major tributary valleys and subsidiary mountain ranges. The Dischma Valley is a small Alpine end valley of 15-km length, 1000-m depth, and 4-km width. The Brush Creek valley is a 25-km long, 650-m-deep, 4-km-wide (ridge-to-ridge) end valley. The Akaigawa Basin is a 10-km wide near-circular basin with a rather flat 5-km-wide floor, and with surrounding peaks of 250-m height. The Aizu Basin is a large elongated basin of 130-km length with a mean depth of about 1000 m. References to studies of these valleys and basins are made with the understanding that the results come from the respective authors' works.

In the well-drained Brush Creek valley, atmospheric cooling rates are relatively small. During the bulk of the nighttime period (2300–0600 MST), they are near 0.2 K h^{-1} when averaged over the valley depth. In closed basins where advection into or out of the basin is precluded, larger rates of cooling can be expected. For example, in the Akaigawa Basin, tethered balloon profiles showed mean nighttime cooling rates after 2100 h of about 0.5 K h^{-1}.

Observations in the Aizu Basin, the Akaigawa Basin, and the Brush Creek valley show that nighttime ground heat fluxes can largely counter longwave net radiation losses so that nighttime sensible heat fluxes are small (0 to 35 W m^{-2}). This conclusion is also supported by the Alpine data of Halbsguth et al. (1984) and Vergeiner and Dreiseitl (1987) in Figs. 2.15 and 2.16 where sensible heat fluxes are near zero or, even, upward into the atmosphere on the mornings of 6 August and 7 September. Evening observations in both valleys show sensible heat fluxes toward the ground at rates near 15 W m^{-2}. Observations in the Brush Creek valley and the Aizu Basin, however, indicate that sensible heat fluxes are generally smaller on the valley floor than on the sidewalls. This could be caused by several factors. First, the valley floor is typically more moist than the sidewalls, so that latent and ground heat fluxes may be relatively more important than radiative and sensible heat fluxes. Second, net radiative losses at lower altitudes in the valley are decreased somewhat by the sky view factor effect described previously. Third, downslope flows on the sidewalls generate shear and turbulence in a shallow layer that would enhance the turbulent sensible heat flux on the sidewalls relative to the valley floor.

In the Aizu and Akaigawa basins, continuous nocturnal cooling occurred with near-zero sensible heat fluxes at the basin floors, suggesting that the cooling was caused by advection of air cooled on the surrounding sidewalls where sensible heat fluxes were apparently larger, although unmeasured. Advective terms are strong, as well, in well-drained valleys such as the Inn and Brush Creek valleys. The calculation of cooling contributed by along-valley advection is prone to experimental errors because of weak along-valley potential temperature gradients. In the 1984 Brush Creek valley experiments, the gradients $(\partial\theta/\partial s)$ were on the order of 0.2 K km^{-1}. In the Inn Valley, the nighttime gradients were near 0.1 K km^{-1}, although aircraft measurements during daytime showed gradients of only 0.03 K km^{-1}.

Daytime energy budgets are not discussed in detail because generalizations are not yet warranted from the small amount of research material so far available. Several findings seem important, though. The Inn Valley research of Freytag (1985) shows that the heat budget can be complicated in large valleys by the large phase shift (up to 5 h) between the diurnal heating cycle and the along-valley wind system. Further, the Dischma Valley and Aizu Basin research has shown that daytime heating may not be confined to the valley atmosphere, so that computations must be extended above the valley and must be corrected for above-valley advective effects. Daytime heating rates in the moist Dischma Valley were small (0.5 K h^{-1}), and the role of advection was rather inconsequential relative to sensible heat flux convergence. Further, the distribution of surface cover appeared to produce spatial variations in sensible heat flux. Regions of heat surpluses and deficits within the valley were expected to transfer heat from the sunny to the shaded sidewall, from the end to the entrance of the valley and, after noon, from the valley to the surrounding region. Finally, in the Aizu Basin, the observed increase in energy storage over the center of the basin appeared to be caused by subsidence warming as a compensation for upslope flows that formed over the valley sidewalls.

2.2.4.3. MOMENTUM BUDGET

An atmospheric momentum budget was completed for a 30-h period during March 1982 for the Inn Valley using data from the MERKUR experiment (Freytag 1986). Pressure gradient and friction were the most important terms in the u-momentum equation. The pressure gradient decreased linearly from the surface to the 1000-m ridgetop, while friction decreased linearly from the surface to 400 m. Diurnal accelerations produced by the pressure gradient term reached 3 m s^{-1} h^{-1} during daytime and -4 m s^{-1} h^{-1} at night. The friction term had the same shape and roughly the same amplitude as the pressure gradient term, but lagged by 1 to 2 h. Actual accelerations and decelerations of the along-valley winds lagged the pressure-gradient zero crossings by 5 to 6 h. The 1- 2-h lag of the friction term is a measure of the reaction time of the wind systems to the forcing pressure gradient. For comparison, calculations by Hennemuth (1986) in the smaller Dischma Valley resulted in a reaction time of only 30 min, and Vergeiner et al. (1987) estimated a value of 8 min for the Brush Creek valley. Freytag (1986) found that the momentum advection terms played a role in damping the wind field of the Inn Valley. Horizontal advection was usually advection of air with less momentum. The role of vertical advection was small, but was most significant in the upper levels of the valley's atmosphere where sinking motions imported slower moving air from above.

2.2.4.4. HUMIDITY BUDGET

A valley moisture budget was completed for two daylight periods in August 1980 in Switzerland's Dischma Valley as part of the DISKUS experiment (Hennemuth and Neureither 1986). This appears to be the only valley humidity budget accomplished to date. Evaporation was the source of water vapor in the valley atmosphere during daylight hours. Vertical turbulent transport accounted for only a minor export of humidity from the valley. The observed morning humidity decrease and afternoon increase were attributed to advection in the local wind systems, with the drainage winds exporting humidity in the morning and the up-valley winds importing humidity in the afternoon. Humidity transport between valleys was thought to be important.

2.3. Slope wind systems

Slope wind systems are driven by buoyancy forces and are formed on any slope where a layer of air adjacent to the slope is either cooled or warmed relative to air at the same level in the ambient environment away from the slope. Slope flows occur quite frequently over sloping terrain of different scales, since thermal boundary layers form daily over most land areas. Slope flows are known on various scales, occurring over large sloping land areas such as Antarctica, where katabatic or downslope winds may reach gale force on the periphery of the continent. We confine our discussion to slope flows occurring on the slopes of isolated mountains and on valley sidewalls. Such slope flows are subject to local terrain, vegetation, and soil moisture influences, are intermittent in time, and may change over short distances (Vergeiner 1982).

2.3.1. Simple slope flows

Mahrt (1982) investigated modeling and observational studies of downslope flows and pointed out, on the basis of a careful scale analysis of the momentum equation, the many different types of downslope flow regimes that are possible. A useful summary of the application of the thermodynamic energy equation in the valley and slope flow layers has been recently provided by Brehm (1986).

The system of equations generally used for slope flows on simple slopes is written in a natural coordinate system oriented along (s) and perpendicular (n) to a slope of constant inclination angle α. The system of equations includes the s- and n-momentum equations, the thermodynamic energy equation, and the continuity equation, respectively, as described by Horst and Doran (1986):

$$\frac{\partial u}{\partial t} + u\frac{\partial u}{\partial s} + w\frac{\partial u}{\partial n} = -\frac{1}{\rho_0}\frac{\partial (p - p_a)}{\partial s} - g\frac{d}{\theta}\sin\alpha - \frac{\partial \overline{u'w'}}{\partial n} \quad (2.20)$$

$$\frac{\partial w}{\partial t} + u\frac{\partial w}{\partial s} + w\frac{\partial w}{\partial n} = -\frac{1}{\rho_0}\frac{\partial (p - p_a)}{\partial n} + g\frac{d}{\theta_0}\cos\alpha \approx 0 \quad (2.21)$$

$$\frac{\partial \theta}{\partial t} + u\frac{\partial \theta}{\partial s} + w\frac{\partial \theta}{\partial n} = -\frac{1}{\rho_0 c_p}\frac{\partial R}{\partial n} - \frac{\partial \overline{w'\theta'}}{\partial n} \quad (2.22)$$

$$\frac{\partial u}{\partial s} + \frac{\partial w}{\partial n} = 0. \quad (2.23)$$

Symbols u and w represent flows down and perpendicular to the slope, and R is the upward flux of net all-wave radiation. The potential temperature stratification is given by

$$\theta = \theta_0 + \gamma z + d(s, n, t), \quad (2.24)$$

where γ is the ambient potential temperature gradient, d is the potential temperature excess near the slope (this will be negative for downslope flows), and θ_0 and ρ_0 are reference values for potential temperature and density in

the absence of surface cooling. The ambient pressure p_a is determined from the formula

$$\frac{\partial p_a}{\partial z} = -\rho_a g, \tag{2.25}$$

where ambient air density is a function of ambient potential temperature, as defined by $\theta_a = \theta_0 + \gamma z$. Equation (2.21) assumes that accelerations perpendicular to the slope are negligible so that the slope flow is in hydrostatic balance normal to the slope.

Following this system of equations, the driving force for the downslope flow is the buoyancy force generated by cooling of the layer adjacent to the slope, as represented by the second term on the right-hand side of (2.20). This force is balanced by the divergence of the turbulent momentum flux (third term), and the adverse pressure gradient associated with the change of depth of the slope flow layer with downslope distance (first term). The temperature deficit develops as a result of radiative and turbulent sensible heat flux divergences, following (2.22).

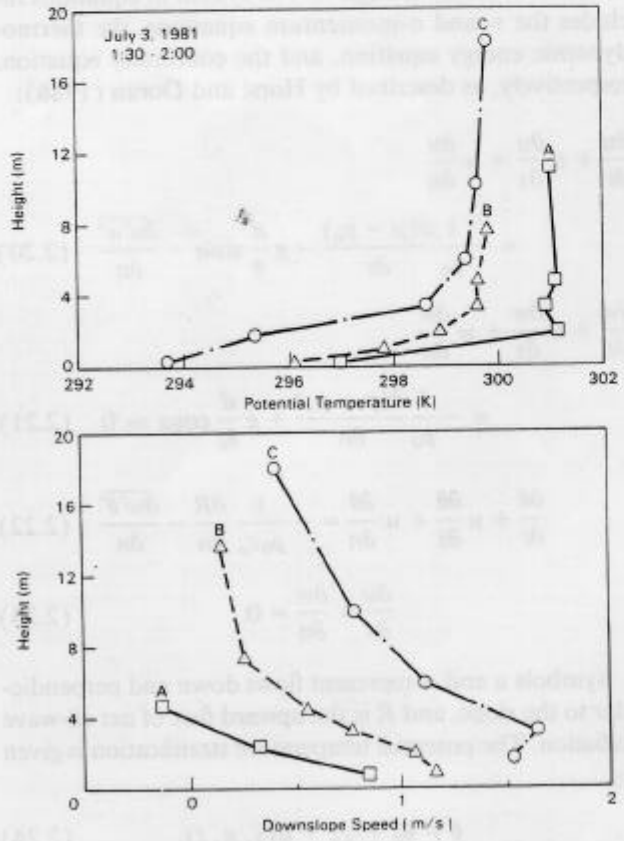

FIG. 2.20. Temperature and wind profiles over the slope of Washington's Rattlesnake Mountain illustrating the evolution of profiles with downslope distance. The upper slope of the mountain is 21° until just below tower B, where it changes to 8°. Ambient winds had upslope and cross-slope components of 1 to 2 m s^{-1}. Reprinted by permission of Kluwer Academic Publishers. (Horst and Doran 1986.)

A large number of slope flow models have been developed over the years, but there have been few datasets that could be used for comparison with simulations. Two datasets collected recently on simple slopes have alleviated this problem somewhat, although the datasets cannot be considered comprehensive because of the lack of surface energy budget and radiation measurements. Horst and Doran (1982, 1986, 1988) have collected slope flow observations on the side of Rattlesnake Mountain, Washington, while Clements and Nappo (1983) developed a similar dataset on the side of Pajarito Mountain, New Mexico. At the Rattlesnake Mountain site, downslope winds did not form regularly from night to night, being quite subject to the prevailing winds and, apparently, to variations in the surface energy balance. Figure 2.20 shows observations of wind and temperature structure as a function of downslope distance on a good drainage night. The topmost tower on the slope, located 69 m below the ridge crest, was designated tower A. Tower B was located 151 m below the ridgecrest and tower C was located 229 m below the ridgecrest.

The shallow inversion over the slope increased in depth with downslope distance, while the drainage flow became stronger and deeper and the height of the peak speed increased. Inversion strength did not change significantly along the slope's length. According to Horst and Doran (1986) the development of the drainage flow with downslope distance was predicted well by Manins and Sawford's (1979b) drainage flow model, except that the inversion strength in the downslope flowing layer did not decrease with downslope distance.

2.3.2. *Slope flows on valley sidewalls*

Downslope flows on valley sidewalls can be expected to differ from flows on simple slopes because of two main factors—one dealing with atmospheric stability and one dealing with ambient winds. The formation and growth of a surface-based inversion over the valley floor ensures that the temperature structure of the ambient environment will undergo temporal changes as the inversion deepens. Potential temperature gradients in the valley inversion typically become weaker with altitude, so that downslope increases in ambient stability are expected. These stability variations in the ambient atmosphere can be expected to organize the slope flow structure in ways that differ from the slope flow structure over simple slopes where ambient stability may vary weakly with altitude. Second, along-valley circulations can be expected to influence the structure and evolution of the shallow downslope flow layer over the slope. Many investigators have previously remarked on the difficulty of finding pure downslope flows on valley sidewalls because of the overriding influence of the down-valley flows (e.g., Hennemuth and Schmidt 1985).

A recent experiment (Doran et al. 1989) investigated the development of downslope flow on a sidewall of the 225-m deep Touchet Valley in Washington. This valley had a uniform sidewall angle of 23 degrees. Three towers, designated A, B, and C, were installed on the fall line of this slope at positions 75 m, 125 m, and 175 m below the ridge crest, respectively. The development of wind and temperature profiles above the slope was monitored by instruments placed on the towers, while changes in the ambient (valley) environment were monitored with tethered balloon and Doppler sodar observations over the valley floor. Results are summarized in Table 2.7. The variation of inversion depth, inversion strength, and buoyancy deficit with distance along the sidewall are summarized in the table. The first column gives predictions of the Manins and Sawford (1979b) model for a simple slope (i.e., a slope on the side of an isolated mountain) in which ambient inversion strength does not vary along the slope. The second column summarizes Horst and Doran's (1982) measurements over the simple slope of Rattlesnake Mountain, and the final column summarizes Doran et al.'s (1989) observations over the sidewalls of the Touchet Valley. The notation A > B for inversion depth, for example, means that inversion depth is greater at tower A than at tower B. Simple slope predictions agree well with observations except for inversion strength, as mentioned previously. Observations on the valley sidewall, however, are at odds with simple slope observations and predictions. These results have been attributed by Doran et al. (1989) to increases in the stability of the ambient environment with downslope distance and to the effects of ambient (down-valley) winds on the downslope layer. Variations in surface energy budget along the slope may also be a contributing factor.

The effects of ambient stability on downslope drainage flows are further illustrated in Fig. 2.21. Here, a succession of pictures shows the dispersal of a smoke plume released into a shallow downslope flow on the upper east sidewall of Colorado's Brush Creek valley, as described by Thorp and Orgill (1986). The upper half of the valley atmosphere on this night was nearly isothermal, with a strong inversion in the lowest 150 m of the valley. The smoke tracer cascaded over a cliff at the head of the box canyon tributary, was carried down the slope of the tributary and, as the slope flow encountered strong ambient stability, the plume became detached from the sidewall and left the sidewall to attain its buoyancy equilibrium level in the valley inversion. It turned the corner of the tributary and was then transported in the Brush Valley down-valley flow. This sequence of events illustrates several points. The flow of the oil fog plume down the cliff requires that a sufficient buoyancy deficit exist in the flow as it approaches the cliff. Further, an accurate model of the slope flow must incorporate the cooling of the parcel during its downslope transport caused by downward sensible heat flux to the underlying ground, warming caused by subsidence, entrainment of ambient air into the slope flow layer, and the effects of the ambient stability. These factors, and the slope angles, may change frequently along the parcel path so that the parcels' equilibrium is continually disturbed. The adequate incorporation of such disparate processes represents a significant challenge to the development of a realistic model.

TABLE 2.7. Relative values of inversion depths, inversion strengths, and buoyancy deficits from predictions for a simple slope, measured on a simple slope, and measured on a valley sidewall (Doran et al. 1989).

	Model prediction	Simple slope	Valley sidewall
Inversion depth	A < B < C	A < B < C	A > B ~ C
Inversion strength	A > B > C	A ~ B ~ C	A ~ B > C
Buoyancy deficit	A < B < C	A < B < C	A > B > C
Katabatic wind	A < B < C	A < B < C	B > A ~ C

Daytime, upslope flows on valley sidewalls have not yet been investigated in detail. In particular, the variation in structure with upslope distance has received little observational attention. Vergeiner predicted (Vergeiner 1982; Vergeiner and Dreiseitl 1987), on the basis of a simple slope layer energy budget, that flow in the layer will be quite sensitive to ambient temperature structure, and that upslope volume flux may decrease or increase with upslope distance depending on the presence or absence of strong stability layers in the ambient environment. Actual observations at a particular location on a slope may be quite unrepresentative of the mean conditions over the slope because of the known inhomogeneity and nonstationarity of these flows in real topography. Dynamic modeling of idealized sidewall topography supports Vergeiner's view of the nonstationarity of the flows as well as the sensitivity of the flows to ambient stratification (Bader and McKee 1985). On the other hand, it may not be necessary to know the detailed turbulent structure of the upslope flows to determine bulk valley warming or bulk changes in the along-valley flows. Such changes are caused by the total energy input to the valley volume and its distribution through the valley atmosphere by the integrated slope flows. Brehm (1986) has recently developed a modeling approach that couples the structure and evolution of sidewall slope flows with the developing structure of the ambient valley temperature structure. This approach has been extended to three dimensions by Egger, Chapter 3.

February observations of temperature structure evolution over a deep snow cover in Colorado's Yampa Valley have suggested that upslope flows are present even in win-

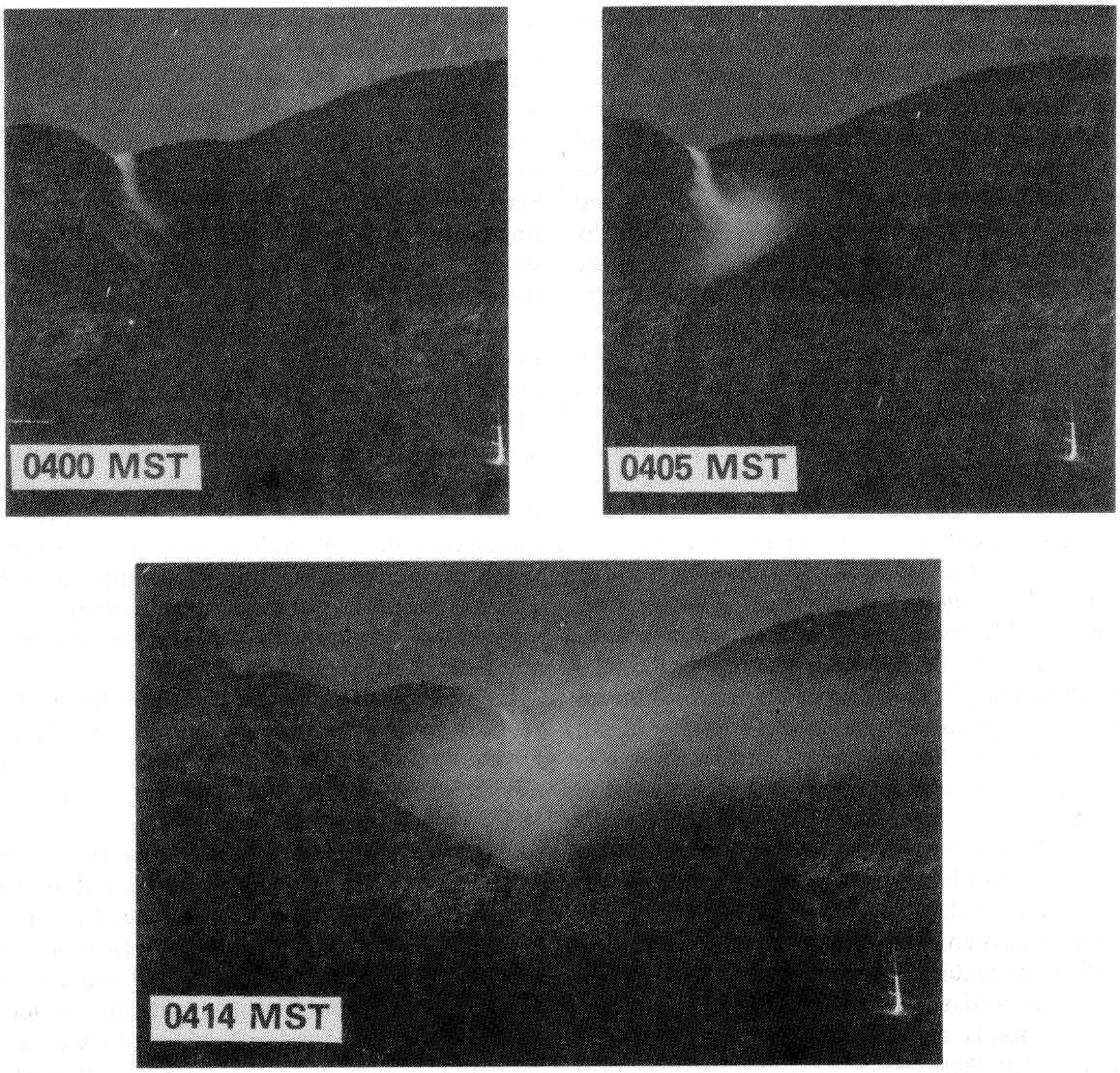

FIG. 2.21. A smoke plume released on the mesalike ridgetop of Colorado's Brush Creek valley was carried over a cliff into a box canyon tributary and down the sidewall until separating from the sidewall and flowing out into the main valley as an elevated plume. (Photographs provided by J. M. Thorp and M. M. Orgill, Battelle NW Laboratories, Richland, Washington.)

ter. Effective heat transfer to the air by the evergreen forests is thought to be the means by which such flows are developed, as illustrated in Fig. 2.22. Special opportunities to compute valley atmospheric energy budgets are present in such conditions that have, as yet, been unrealized. Ground and latent heat fluxes at the surface [see Eq. (2.15)] may be negligible in such conditions because of the insulating effect of the snow cover and the subfreezing temperatures. Further, on days when air temperatures rise above freezing, the direction of the sensible heat flux will be affected by the inability of the snow surface temperature to rise above 0°C.

The superposition of the valley and slope wind systems results in a diurnal turning of the wind over the sidewalls, as shown in Fig. 2.23, so that, regardless of valley orientation, winds on the left sidewall of a river valley (taking the river's point of view) turn counterclockwise with time, while winds on the right sidewall turn clockwise with time. This turning is illustrated with data for the opposite sidewalls of Colorado's Brush Creek valley in Fig. 2.24.

2.4. Morning transition

Early observations of valley temperature structure evolution (Ekhart 1948, 1949; Machalek 1974) showed that a typical feature of the morning transition period was the descent into the valley of the top of the nocturnal temperature inversion. Pibal wind observations collected by other observers (Ayer 1961; Davidson and Rao 1963) showed a similar feature in the wind observations. After

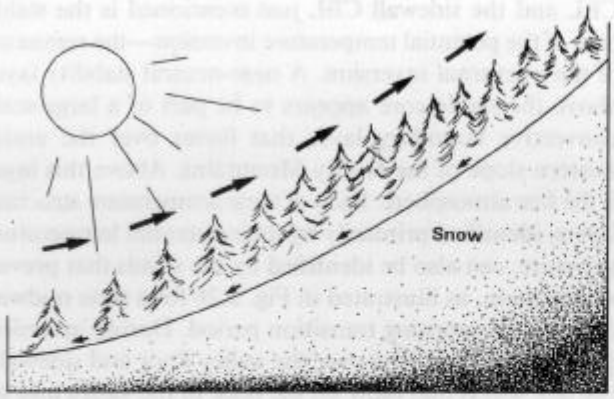

FIG. 2.22. Upslope flow can form over a forested slope in winter even when the ground is covered with snow. (Adapted from Hawkes 1947.)

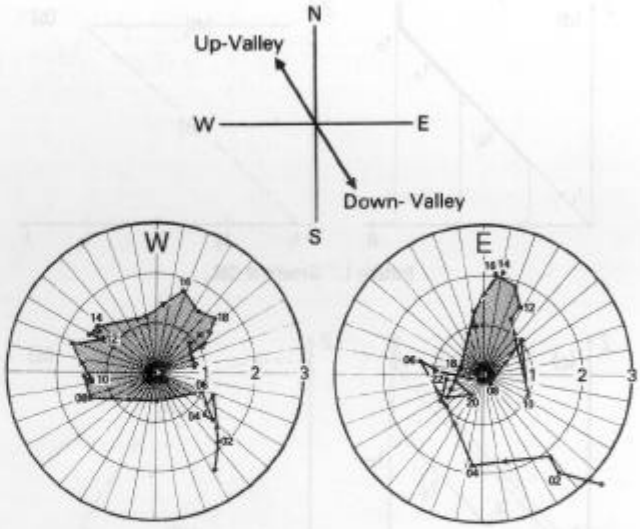

FIG. 2.24. Wind hodographs for the opposing sidewalls of Colorado's Brush Creek valley, 25 September 1984. (Whiteman et al. 1989b.)

sunrise, the winds within a valley would continue to blow down the valley, but a wind reversal (to up-valley) would first occur aloft and the wind reversal point would descend into the valley with time.

Interpretations of the cause of the descent phenomena were hampered by a lack of good data; especially critical was the need for concurrent wind and temperature structure data in a number of valleys. Initial hypotheses attributed the descent of the wind reversal point and the (assumed) top of the temperature inversion to "turbulent erosion" by strong winds aloft (Davidson and Rao 1963) or the draining of the nocturnal valley cold air pool down the valley's axis after sunrise (Ayer 1961).

Analysis of observations taken in the late 1970s in a number of Colorado valleys (Whiteman 1980, 1982) has provided an explanation for the inversion descent phenomenon that emphasizes the role of subsidence in the valley atmosphere in effectively transferring heat received at the slopes to the entire valley cross-section.

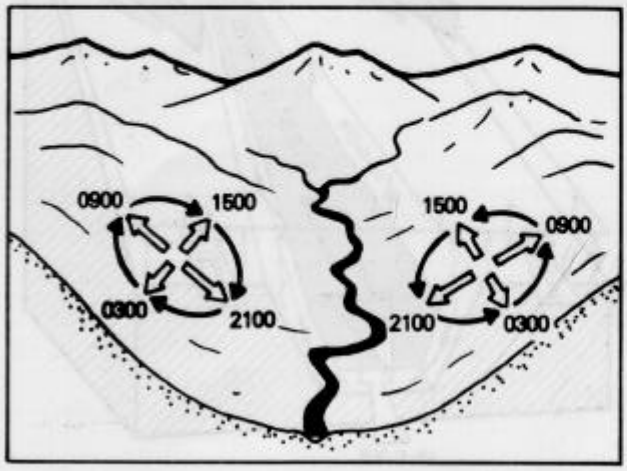

FIG. 2.23. Winds on the left bank of a river (i.e., right side of the figure) turn counterclockwise with time; winds on the right bank turn clockwise. (Adapted from Hawkes 1947.)

Temperature inversions in the Colorado valleys typically developed to the full depths of the valleys and were destroyed after sunrise following one of three patterns of temperature structure evolution (Fig. 2.25). The first pattern, observed in the widest valley studied, approximates inversion destruction over flat terrain, in which the nocturnal inversion is destroyed after sunrise by the upward growth from the ground of a warming convective boundary layer (CBL). The second pattern, observed in snow-covered valleys, differs significantly from the first. Here the growth of the CBL, which begins after sunrise, is arrested once the CBL has attained a depth of 25 to 50 m. The inversion is then destroyed as the top of the nocturnal inversion descends into the valley. Successive profiles of the valley atmosphere show a warming consistent with a simple subsidence of the previous profiles. The third pattern of temperature structure evolution was observed in all of the valleys when snow cover was not present and describes the majority of case studies observed in field experiments. Following this pattern, inversions are destroyed by two processes: the continuous upward growth from the valley floor of a warming CBL and the continuous descent of the top of the nocturnal temperature inversion. Warming of the elevated inversion layer above the CBL is consistent with a simple subsidence of the previous profiles. In the Colorado valleys studied, the time required to break an inversion and establish an unstable atmosphere within the valley was typically $3\frac{1}{2}$ to 5 h after sunrise. Temperature structure evolution during clear, undisturbed weather differed little from day to day and from season to season. Further, the valley inversions

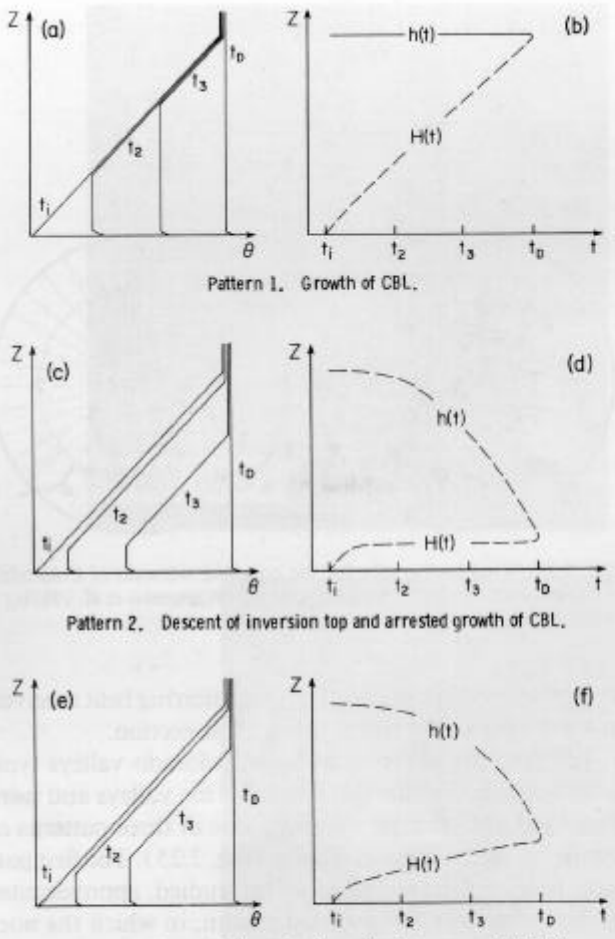

FIG. 2.25. Summary of the three different types of inversion breakup observed in Colorado valleys. Pattern 1 is the pattern typically seen over flat plains and occurs in very wide valleys, pattern 2 occurs in snow-covered valleys, and pattern 3 occurs in most non–snow-covered valleys. (Whiteman 1982.)

showed less variability from day to day and from season to season than inversions over the adjacent plains (Whiteman 1982). This suggests that, at least for a narrow range of weak to moderate synoptic flow conditions investigated, deep valley topography produces more consistent inversions by protecting them from winds aloft.

The common element of all three patterns of temperature structure evolution is the development of a CBL over the valley floor after it is illuminated by direct sunlight. Observations of the sidewall of one of the valleys indicate that a CBL begins to grow above the sidewall after direct sunlight illuminates it. The temperature structure of the sidewall CBL is similar to that of the CBL over the valley floor, but upslope winds blow at speeds up to 3 m s^{-1} in the sidewall CBL.

The Colorado observations have indicated that five different temperature structure layers may be present during the inversion destruction period. Above the valley floor CBL and the sidewall CBL just mentioned is the stable core of the potential temperature inversion—the remnants of the nocturnal inversion. A near-neutral stability layer above the stable core appears to be part of a large-scale convective boundary layer that forms over the entire western slope of the Rocky Mountains. Above this layer is the free atmosphere. Each of these temperature structure layers, identified primarily by their potential temperature structure, can also be identified by the winds that prevail within them, as illustrated in Fig. 2.26 for a time midway through the morning transition period. During inversion destruction, the CBLs over the valley floor and sidewalls contain winds that blow up the floor of the valley and up the slopes. The CBL, or neutral layer, above the valley inversion has winds that blow up the inclined western slope of the Rocky Mountains during the day. Winds in the stable core typically continue to blow down-valley after sunrise until the stable core is nearly destroyed. Winds in the stable free atmosphere may blow from any direction with speeds determined by synoptic-scale pressure gradients. Despite some variability in the strength and timing of reversal of the winds, the temperature structure evolves uniformly from day to day in individual valleys.

A hypothesis was developed to explain the observed temperature structure evolution (Fig. 2.27). Initially, just before sunrise, a deep temperature inversion fills the valley. After sunrise, solar radiation received on the valley floor and sidewalls is partly converted to sensible heat flux. Sensible heat flux causes a CBL to develop over the

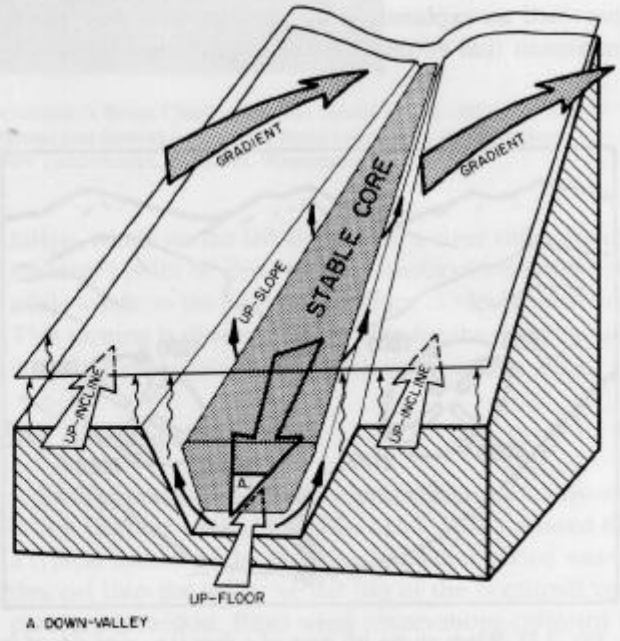

FIG. 2.26. View of the interacting wind systems during the inversion breakup period. (Whiteman and McKee 1982.)

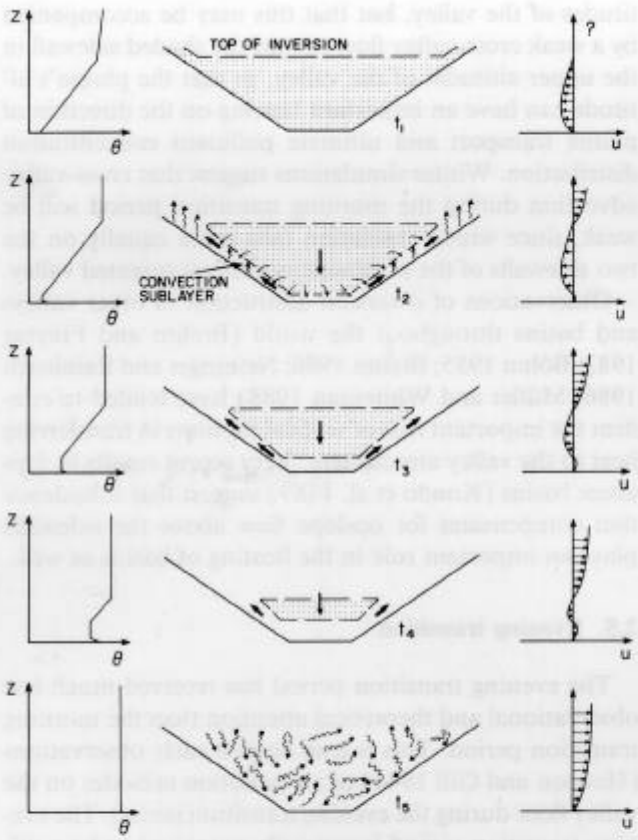

FIG. 2.27. Inversion breakup hypothesis. Stable core air is entrained into the convection sublayer and removed from the valley in upslope flows, producing a compensating subsidence over the valley center. In the center of the diagram cross sections of a valley are shown at times t_1, t_2, t_3, t_4, and t_D. On the left are corresponding potential temperature profiles as taken from the valley center. On the right are corresponding up-valley wind components as a function of height. At sunrise, t_1, an inversion is present in the valley. At t_2, a time after sunlight has illuminated the valley floor and slopes, a growing CBL is present over the valley surfaces. Mass and heat are entrained into the CBLs from the stable core above and carried up the sidewalls in the upslope flows. This results in a sinking of the stable core and growth of the CBLs (t_3 and t_4) until the inversion is broken (t_D) and a turbulent well-mixed neutral atmosphere prevails through the valley depth. Down-valley winds continue to blow in the stable core during the inversion breakup period. Winds in the CBL below, and in the region above the stable core, often blow up-valley during this same period. (Whiteman 1982.)

surfaces. Mass is entrained into the CBLs from the stable core above and carried from the valley in the upslope flows that develop in the CBLs over the sidewalls. This removal of mass from the base and sides of the stable core causes the elevated inversion to sink into the valley and to warm adiabatically as a result of subsidence. Incidentally, the subsidence (or, equivalently, the mass flux divergence from the CBLs) decreases the rate of growth of the CBLs over the valley floor and sidewalls relative to normal CBL growth rates over flat plains.

The physical concepts applied here are quite closely related to concepts discussed in earlier sections of this chapter. The valley atmosphere is driven by incoming solar radiation. Some of the radiation, when received on the valley surfaces, is converted to sensible heat flux. The topographic amplification factor plays an important role in determining the rate of warming of the valley atmosphere for a given energy input. Vertical convergence of sensible heat flux over the sidewalls warms the inclined CBL. An upslope flow quickly develops in this layer. Transport of mass by upslope flows requires compensatory subsiding motions over the valley's center. This subsidence in the stable valley atmosphere produces warming and provides a very effective mechanism for transporting the energy received at the valley sidewalls throughout the entire valley atmosphere. The warming of the valley atmosphere, enhanced by the topographic amplification factor, decreases the nighttime along-valley pressure gradient and eventually causes the down-valley winds to reverse. When the elevated remnant of the nocturnal inversion is finally destroyed, continued upslope flow will fail to produce compensatory warming in the valley center because the vertical potential temperature gradient vanishes. Much of the energy is then transported from the valley and goes to develop CBLs above the mountain range.

A thermodynamic model based on a simplified energy budget of the valley atmosphere and incorporating a topographic amplification factor (Whiteman and McKee 1982) can adequately describe the evolving temperature structure during the inversion breakup period in typical valleys. The model, however, requires the specification of a free parameter indicating the fraction of the sensible heat flux to be used for CBL growth, with the remaining fraction used for transporting mass up the sidewall and producing compensatory subsidence and warming over the valley center. Further research is necessary to gain a better understanding of the factors that affect the partitioning of energy in actual valleys, and thus affect the pattern of inversion destruction to be followed (Fig. 2.25). Observations show that high rates of input of sensible heat flux into the valley atmosphere favor the growth of convective boundary layers and pattern 1 inversion destruction. This pattern is also favored in wide valleys [e.g., the wide South Park valley investigated by Banta and Cotton (1981)], where compensatory subsidence is weak because the upslope flows carry small amounts of volume relative to the total atmospheric volume in the cross section. Pattern 3 is the most common pattern of temperature inversion destruction in valleys since inversions are typically destroyed by a combination of CBL growth and subsidence warming, but changes in the surface energy budget in a given valley from day to day (say, following a rain) have an effect on the relative importance of the CBL growth and subsidence warming mechanisms (Whiteman 1982).

Recent work has clarified important aspects of wind and temperature structure evolution during the morning transition period. The relatively minor role played by turbulent erosion at the top of the temperature inversion has been documented in two-dimensional dynamic model simulations by Bader and McKee (1983). Further, their simulations have shown that variations in albedo on a valley cross-section can make important changes in the inversion destruction pattern followed. Gravity waves play an important role in transferring heat across the valley atmosphere when differential heating occurs on the opposite sidewalls (Bader and McKee 1985). Further, the dynamic model simulations show that the upslope flows are not necessarily continuous along the slope and are quite nonstationary. The noncontinuous slope flows were predicted independently by Vergeiner (1982) based on an energy budget equation that he developed for the slope flow layer. Small-scale topographic features on the slopes as well as ambient atmospheric layers of intense stability may cause mass to leave the slope and converge into the valley atmosphere, carrying its heat content, and producing organized large-scale cross-valley circulations. Brehm (1986) has carried Vergeiner's energy budget approach further and developed a model of temperature structure evolution that explicitly includes the evolution of the slope flow layer and allows the along-slope volume flux to converge or diverge depending on ambient atmospheric stability. His comparison of the model with data suggests that the direct heating of the valley atmosphere through mass leaving the slope is small compared to subsidence warming.

Dispersion of elevated nocturnal pollutant plumes in valleys is strongly affected by inversion breakup processes, and high ground-level pollution concentrations have been frequently observed during the morning transition period (e.g., Hewson and Gill 1944). When valleys are oriented in a north–south direction, solar insolation can be quite different on the opposing sidewalls during the morning transition period. If the valley is narrow this can produce significant cross-valley pressure gradients and cross-valley flows (Urfer-Henneberger 1964, 1970). These cross-valley flows may carry elevated air pollution plumes toward the more strongly heated sidewall. There, high concentrations may be experienced as the plume is fumigated into the growing CBL and carried upslope. These physical processes were found to be important contributors to dispersion of elevated tracer plumes in Colorado's northwest–southeast oriented Brush Creek valley in summer and fall experiments (Whiteman 1989; Gudiksen and Shearer 1989). Summer and winter cross-valley advection of elevated plumes in the Brush Creek valley have been simulated recently with a dynamic model (Bader and Whiteman 1989). Summer simulations show that a cross-valley flow toward the heated sidewall occurs in the lowest altitudes of the valley, but that this may be accompanied by a weak cross-valley flow toward the shaded sidewall in the upper altitudes of the valley, so that the plume's altitude can have an important bearing on the direction of plume transport and ultimate pollutant concentration distribution. Winter simulations suggest that cross-valley advection during the morning transition period will be weak, since winter insolation falls more equally on the two sidewalls of the northwest–southeast oriented valley.

Observations of inversion destruction in other valleys and basins throughout the world (Brehm and Freytag 1982; Böhm 1985; Brehm 1986; Neininger and Reinhardt 1986; Müller and Whiteman 1988) have tended to confirm the important role of vertical motions in transferring heat to the valley atmosphere. Very recent results in Japanese basins (Kondo et al. 1989) suggest that subsidence that compensates for upslope flow above the sidewalls plays an important role in the heating of basins as well.

2.5. Evening transition

The evening transition period has received much less observational and theoretical attention than the morning transition period. This is true despite early observations (Hewson and Gill 1944) of air pollution episodes on the valley floor during the evening transition period. The evening transition period is generally perceived to be a difficult observational, theoretical, and modeling problem because of the nonstationary nature of the transition period and the combination of important physical processes acting on multiple time and space scales.

The evening transition period is generally defined as the time period through which daytime up-valley flows are reversed to down-valley flows and attain a reasonably steady state, characteristic of nighttime. Key physical processes during the transition period include the reversal of the sensible heat flux and the development of downslope flows. The spatial pattern of sensible heat flux reversal and the near-coincident slope flow reversal can be quite complicated in a real valley. Sensible heat flux reversal is closely related to the time of local sunset, so that the progression of shadows in a valley can sometimes give an indication of the spatial field of negative sensible heat flux. Downslope flows begin locally after the sensible heat flux reverses (Whiteman et al. 1989b). The air cooled above the sidewalls flows downslope so that the cooling is effectively confined within the valley. Compensatory rising motions over the valley center, which arise as a response to the downslope flows over the valley sidewalls, are thought to contribute to the cooling there. From this, one obtains a picture of nonhomogeneous, nonstationary processes producing cooling within the bulk of the valley atmosphere. One could speculate about the difficulty of obtaining representative measurements of turbulence, etc.,

during this time period. This cooling of the valley atmosphere eventually becomes sufficient to reverse the temperature contrast between valley and plain (or, more properly, along the valley axis) so that the along-valley pressure gradient reverses sign and down-valley winds are initiated.

In addition to the sensible heat flux divergence that produces cooling in a shallow layer above the slopes and the rising motions that produce cooling over the valley center, cooling of the valley atmosphere is also produced by radiative flux divergence and, on a given valley cross-section, may be produced by horizontal down-valley cold air advection. Advective effects could be especially significant if along-valley gradients in sensible heat flux were present along the length of the valley at a given time. This must be a quite frequent occurrence, since such gradients could be produced by differences in shading caused by changes of direction of the valley axis, as well as along-valley differences in soil moisture, vegetation cover, soil conductivity, or other factors affecting the surface energy budget.

Over flat plains, cooling typically begins in a shallow layer near the ground that deepens slowly through the course of the night. In valleys, on the other hand, several mechanisms combine to produce deep cooling through the entire valley atmosphere rather than confining the cooling to a shallow layer at the valley's floor. Further, the topographic amplification factor enhances the total cooling within the valley relative to the plain, since energy losses out the top of the valley come from a smaller volume of air and thus produce larger temperature decreases. An example of such cooling and the corresponding wind structure evolution over a 4-h evening transition period is shown for Colorado's 700-m-deep Eagle Valley in Fig. 2.28. Initial soundings showed that the daytime winds blew up valley, as expected. A shallow down-valley wind layer formed first near the ground and rapidly grew in depth. A shallow transition layer wind is evident at the top of the down-valley wind layer and appears to be at about the same height as a sharp inversion layer. The evolution of peculiar small-scale features in the potential temperature profiles appears to be related to the convergence of downslope flows that leave the sidewalls. The upward propagation of these features suggests that rising motions occur over the valley center as a compensation for downslope flows over the sidewalls, as shown in Fig. 2.29. Further observations will be necessary before this interpretation can be tested.

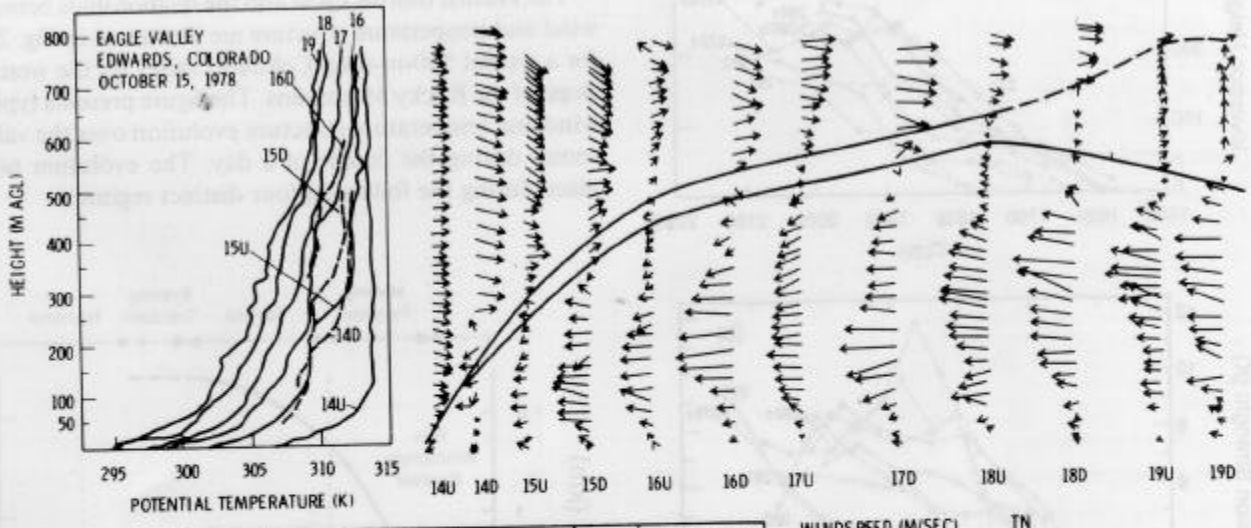

#	TIME (MDT)	#	TIME (MDT)	#	TIME (MDT)
14U	1802-1820	16U	1931-1947	18U	2100-2118
14D	1820-1836	16D	1947-2001	18D	2118-2133
15U	1846-1903	17U	2014-2031	19U	2143-2202
15D	1903-1922	17D	2031-2045	19D	2202-2216

FIG. 2.28. Temperature and wind structure evolution during the evening transition in the 700-m-deep Eagle Valley on 15 October 1978, illustrating the rapid development of the down-valley wind system and the growth of the temperature inversion. Note that small-scale features in the temperature structure are maintained from sounding to sounding. In the figure, vector winds are plotted as a function of height; vector lengths correspond to wind speeds (see wind speed legend). The up-valley direction is given for reference. The time intervals over which the up (U) and down (D) soundings were conducted are given in the table. The solid lines in the wind profiles delineate the boundaries of the wind transition layer. (Whiteman 1986.)

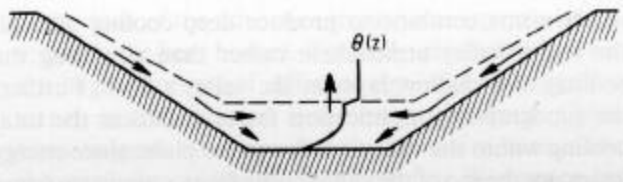

FIG. 2.29. Postulated flow in relationship to temperature inversion features in the previous diagram. Slope flows appear to leave the slope and converge toward the valley center producing compensating rising motions that cool the atmosphere over the valley center.

The rapid development of valley temperature inversions during the evening transition period has been confirmed in recent fall experiments in Washington's 225-m-deep Touchet Valley (Doran et al. 1989). On clear nights in the Touchet Valley, inversions attain the full valley depth within 3 h of the start of inversion formation (Fig. 2.30a); inversion growth is accompanied by an initial rapid growth in inversion strength (potential temperature difference between the ground and the top of the inversion) followed by the gradual attainment of an equilibrium strength of 7 or 8 K (Fig. 2.30b). Loss of energy storage

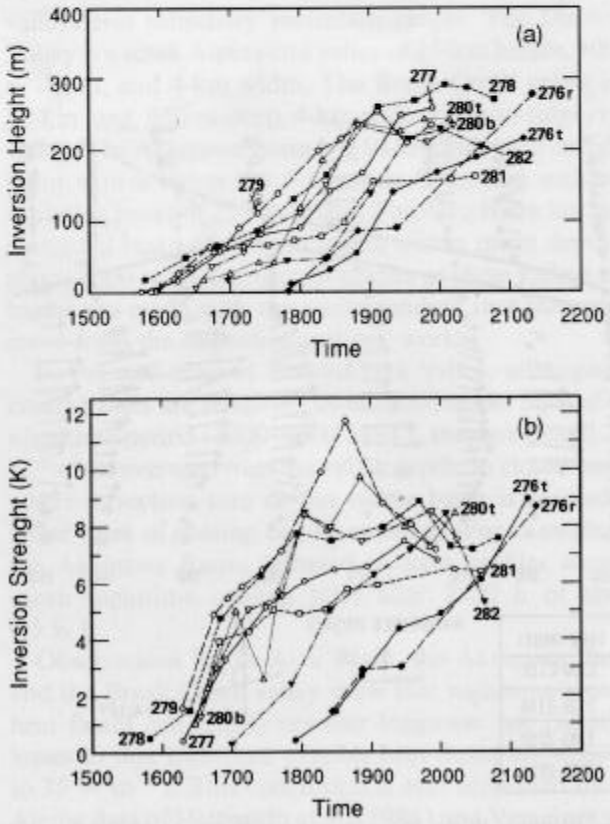

FIG. 2.30. Growth of (a) temperature inversion depth and (b) inversion strength with time in Washington's 225-m-deep Touchet Valley during clear October nights in 1986. Dates given are Julian dates; 4 October is equal to Julian date 276. Dual tethersondes were used at different valley locations on Julian dates 276 and 280. (Doran et al. 1989.)

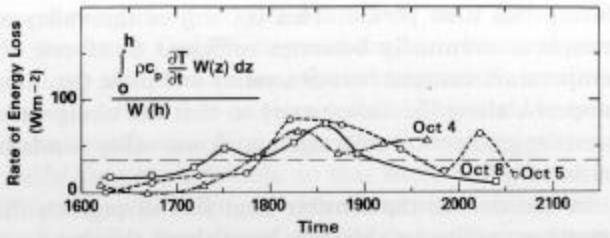

FIG. 2.31. Rate of loss of energy from a unit vertical cross-section of Washington's Touchet Valley in 1986 as normalized by the width of the cross section. The horizontal line provides a rough estimate of the rate of loss of energy that could be explained by diabatic processes in the valley cross-section.

in the valley atmosphere follows the pattern shown in Fig. 2.31, in which valley energy loss (normalized by the cross sectional area of the valley's lid) reaches a peak of 60 to 70 W m^{-2} during the 1730 to 1930 PDT period when the down-valley winds become strong. Estimates of sensible and radiative flux divergences from the valley cross-section suggest that this rapid cooling cannot be explained solely by diabatic processes occurring in the cross section, suggesting that down-valley cold air advection may play an important role during the evening transition period.

2.6. The diurnal cycle

The normal diurnal cycle and the relationships between wind and temperature structure are illustrated in Fig. 2.32 for a typical 500-m-deep Colorado valley on the western slope of the Rocky Mountains. The figure presents typical wind and temperature structure evolution over the valley center during the course of a day. The evolution takes place during the following four distinct regimes:

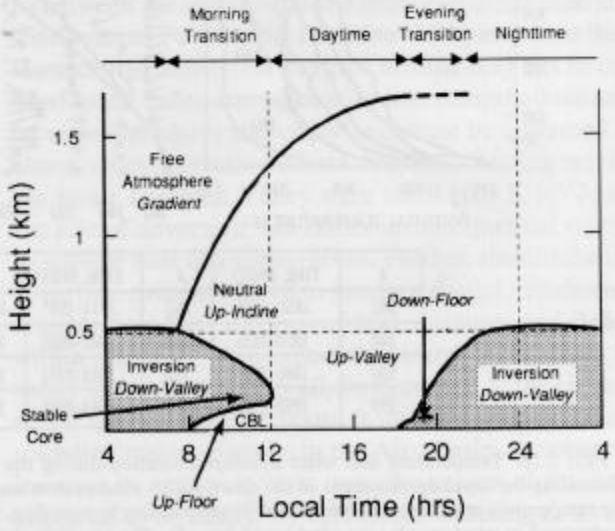

FIG. 2.32. Typical diurnal evolution of temperature (bold) and wind (italics) structure layers in a 500-m-deep valley.

• *Nighttime:* Observations taken over the valley center during the nighttime show that a temperature inversion is generally present, with depth approximately equal to the valley depth. Downslope flows occur on the sidewalls during this period. Down-valley winds prevail within the inversion, but larger-scale pressure gradients produce gradient winds that may blow from any direction in the slightly stable atmosphere above the valley. During this period the valley flows are decoupled from the flows above the valley by the presence of the surrounding ridges and by the stable temperature structure within the valley that suppresses vertical exchange of momentum.

• *Morning transition:* At or shortly after sunrise, convective boundary layers begin to grow above heated surfaces. Over the ridges, a CBL (designated the "neutral layer" in Fig. 2.32 to distinguish it from other convective boundary layers) is produced. Winds in this layer blow up the inclined western slope of the Rocky Mountains. During the morning transition period (and the daytime period, as well) the neutral layer grows into the slightly stable free atmosphere above, which represents the remnant of the previous day's mixing layer. The rate of growth of the neutral layer is high if sensible heat flux is strong since the stability of the ambient atmosphere into which it grows is weak. Over the valley floor and sidewalls, however, convective boundary layers grow slowly upward into the remnants of the strong nocturnal inversion, while the top of the inversion sinks deeper into the valley. CBL growth is slowed by the divergence of mass from the slope boundary layer or, equivalently, by subsidence of the ambient environment. The important role of the upslope flows in heating the valley atmosphere during this period has been previously mentioned. By midday the remnant of the nocturnal inversion within the valley (stable core) is finally destroyed by CBL growth and inversion sinking. The valley atmosphere becomes well mixed, and potential temperature becomes constant with height, although the valley atmosphere continues to warm with time.

• *Daytime:* After the remnants of the nocturnal inversion are destroyed, convection occurs above all of the valley surfaces—valley floor, sidewalls, and ridgetops. Thermally developed winds within the valley blow up the valley and up the slopes, but winds gradually change with height to the wind directions prevailing above the valley. During this period the valley atmosphere may become closely coupled with the atmosphere above the valley by enhanced vertical transfer of momentum. Winds in the valley can become turbulent and upper winds can be channeled into the valley, enhancing or countering the up-valley winds that develop locally. This daytime overpowering of the thermally developed winds is a common feature of meteorology in the western United States and in other areas where deep daytime convective layers may develop. Strong gusty daytime winds may be quite important for air pollution dispersion, prediction of forest fire behavior, etc. In the absence of such winds, the thermally developed daytime up-valley and nighttime down-valley wind systems have about the same strength. This is evidently because the topographic amplification factor becomes ineffective in creating strong along-valley temperature gradients after the valley inversion is destroyed since the incoming energy can no longer be confined within the valley.

• *Evening transition:* The evening transition period begins in late afternoon after cooling over shaded surfaces initiates downslope flows on the sidewalls and valley floor. Once the downslope flows begin, a valley temperature inversion containing down-valley winds grows through the valley depth. Compensatory rising motions over the valley center act to cool the valley atmosphere through its entire depth.

2.7. Other phenomena

2.7.1. Influence of external winds

Because most valley meteorology field experiments to date have focused on periods when upper winds were weak, little evidence has been accumulated on the effects of variable ambient winds on the development of thermally forced local wind systems. Some influence on the local wind system is nearly always present and is more or less manifest, depending on atmospheric stability and the strength and direction of the upper winds or, equivalently, on the above-valley pressure gradients. These pressure gradients may counteract or be superimposed on locally developed pressure gradients. Many mechanisms can be proposed to explain the influence of upper winds on local circulations, but the effects of topography may be difficult to quantify and present observational tools are not readily available for investigating the details of interactions at valley ridgetop levels.

Germany's 35-km-wide, shallow, flat-bottomed, Rhine Valley is quite susceptible to influence from prevailing flows above the valley, but the means by which this influence is felt is somewhat surprising. Under stable conditions, winds within the valley typically blow parallel to the north–south valley's axis, and the direction depends strongly on the direction of the geostrophic wind above the valley at 850 hPa, as shown in Fig. 2.33. Note in the figure that geostrophic winds from the west are most frequently associated with a surface wind from the south and that, when geostrophic winds blow from the south, small changes in direction can result in surface winds in the valley from either south or north. The explanation for this is related to the pressure pattern associated with the geostrophic wind and its superposition on the local pressure pattern in the valley. The geostrophic wind blows parallel to isobars, with higher pressure on the right. Thus,

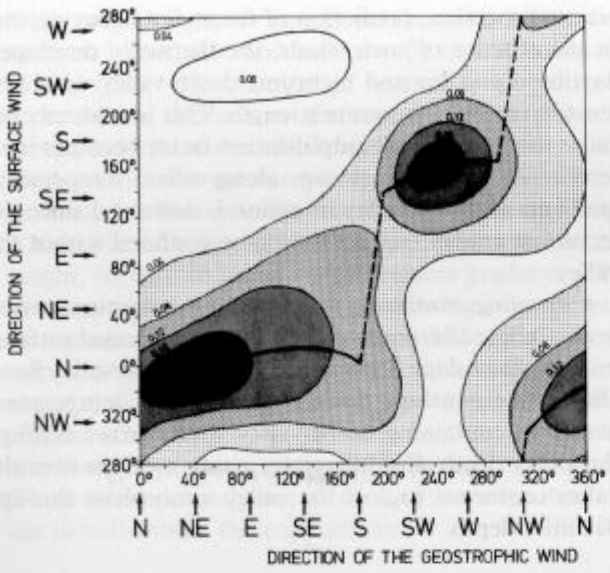

FIG. 2.33. Relative frequency of surface wind directions in the Rhine Valley at Mannheim, Federal Republic of Germany, as a function of geostrophic wind direction. The heavy solid line connects the most frequent wind directions. Data are for the period 1969–74, for stable stratifications only. (Wippermann and Gross 1981.)

westerly geostrophic winds above the valley are associated with a high pressure to the south and a low pressure to the north. The superposition of this large-scale pressure pattern on the valley forces surface winds in the valley to blow from the south—from high to low pressure along the valley channel. This extreme sensitivity of the valley wind system to the large-scale pressure pattern is thought to be a feature of shallow valleys where thermally developed wind systems are weak.

Even in deep valleys, however, such as the valleys in California and Colorado investigated by the ASCOT program, important aspects of the structure of valley circulations can depend on rather subtle differences in ambient atmospheric conditions (Barr and Orgill 1989). In the 1984 ASCOT experiment in Colorado's Brush Creek valley, down-valley drainage flow depth was closely related to the strength of the above-valley ambient flows (Fig. 2.34). When ambient winds were strong, drainage flows were shallow; when ambient winds were weak, drainage flows tended to fill the entire valley depth. Such observations suggest that the degree of influence of ambient flows on valley circulation patterns varies over a wide range, so that it may be inappropriate to speak of the influence as a dichotomous process in which ambient flows are considered either coupled or decoupled. In the 1980 ASCOT experiment in California's Anderson Creek valley, the influence of ambient flows varied from night to night. Strong ambient flows intruded into the valley on two successive nights, disrupting well-established drainage flows (Fig. 2.35).

2.7.2. *Maloja winds*

Occasionally, observations are made of deviant wind systems operating in apparent violation of valley wind theory. The best-known example is the Maloja wind in the upper Engadine Valley of Switzerland near the Maloja Pass. The wind system in the upper section of the valley blows up-valley during nighttime and down-valley during daytime, in apparent contradiction with theory. The accepted explanation is that the wind system from the steep Bergell Valley crosses the Maloja Pass and intrudes into the shallow upper Engadine Valley. The ridgelines of the Bergell extend beyond the pass into the upper Engadine, suggesting that the intrusion may be thermally driven rather than momentum driven. Calculations of topographic amplification factors may thus help to clarify the mechanism for this wind system (Fig. 2.36).

Two valleys draining Mount Rainier, Washington, produce winds of the Maloja type (Buettner and Thyer 1966). These are apparently the only U.S. valleys where such wind systems have been documented, but one could expect more Maloja-type winds to be discovered as further wind systems in the western United States are investigated.

2.7.3. *Jets at valley exits*

The down-valley wind often attains its maximum strength at the valley's exit, or a short distance beyond. Several factors may be responsible for this phenomenon. First, enhanced horizontal pressure gradients occur near the exit because pressure differences there are manifested over shorter length scales. Second, at the valley exit, down-valley accelerations occurring along the valley's length have had the maximum time to act. Finally, a conversion of potential energy to kinetic energy may occur at the valley's exit as the cold valley air sinks and fans out over the plain. These factors would appear to be maximized for deep valleys ending abruptly at the plain, rather than for valleys that become progressively shallower with down-valley distance.

Pamperin and Stilke (1985) report on the strong wind that issues from the mouth of Austria's Inn Valley. The development with time of the nocturnal wind speed profiles over Thalreit, Federal Republic of Germany (located on the southern German plain less than 10 km from the mouth of the Inn Valley) on the night of 25–26 March 1982 is shown in Fig. 2.37. The winds issued directly from the valley exit, with a clear jet profile beginning as early as 2015 UTC. The jet became stronger with time, attaining peak speeds of 14 m s^{-1} by sunrise, with the strongest winds at about 200 m AGL. On the same night, as part of the MERKUR experiment, wind observations were taken at Niederbreitenbach, 20 km up-valley from the valley exit. Along-valley wind components at the two stations are shown in time–height sections in Fig. 2.38.

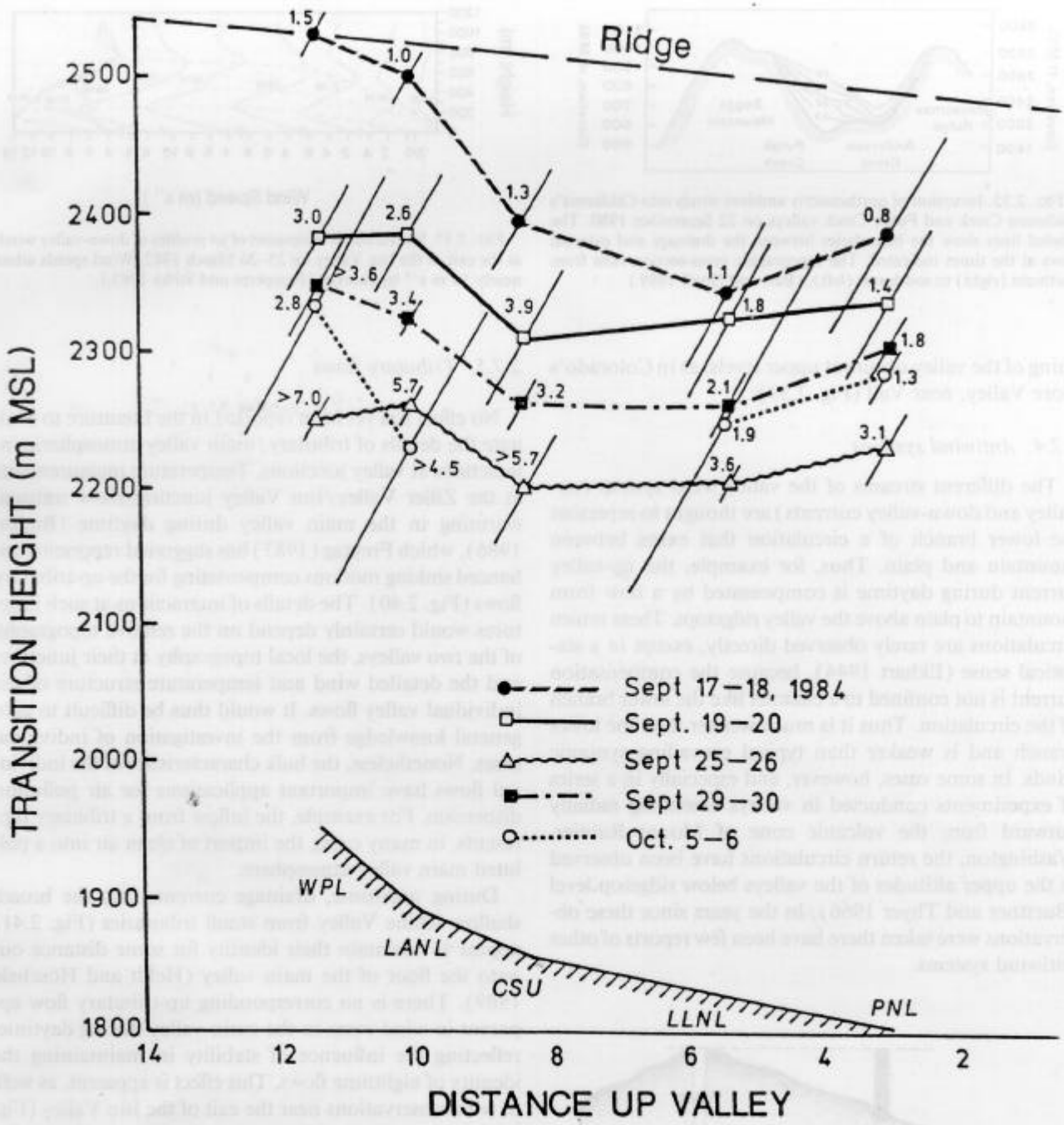

FIG. 2.34. Effect of ambient wind speeds on the height of the transition between the nighttime down-valley flow and the above-valley flow. Data are shown for five nights at various points along the longitudinal axis of Colorado's Brush Creek valley. Numerical data indicate the speed of the above-valley flow (average of the wind speeds in the upper 100 m of the valley atmosphere). The standard deviations of the tethersonde-observed heights are indicated by the inclined lines. (Barr and Orgill 1989.)

Down-valley wind speeds reached 7 m s^{-1} at a height of 625 m inside the valley just before sunrise, but attained speeds of 13 m s^{-1} at a height of 200 m beyond the valley exit. Similar jet profiles have been observed at the mouths of other Alpine valleys—at the south of Lago Maggiore, Italy, near Salzburg, Austria, in the Loisach Valley below Garmisch, Federal Republic of Germany, and in the Beierbach Valley, Austria. The author has seen similar nighttime winds at Paonia, Colorado, where the valley of the North Fork of the Gunnison River fans out into a wide plain.

Elevated jets are sometimes found in valleys where a constriction in the lower altitudes of the valley causes pooling of air in the lowest layers, but a significant wid-

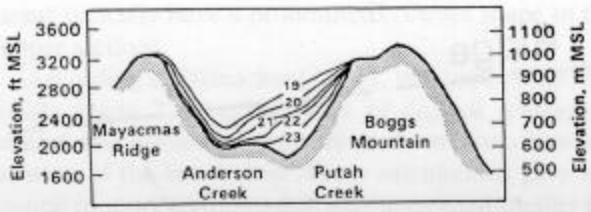

FIG. 2.35. Incursion of northeasterly ambient winds into California's Anderson Creek and Putah Creek valleys on 22 September 1980. The labeled lines show the boundaries between the drainage and external flows at the times indicated. The topographic cross-section runs from northeast (right) to southwest (left). (Barr and Orgill 1989.)

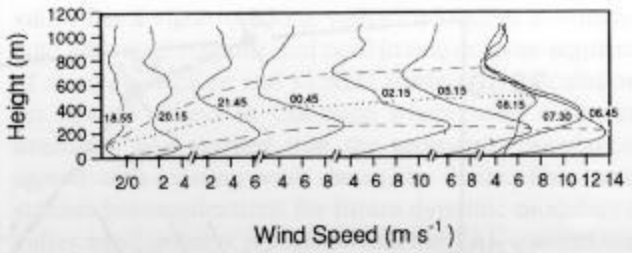

FIG. 2.37. Nocturnal development of jet profiles of down-valley winds at the exit of the Inn Valley on 25–26 March 1982. Wind speeds attain nearly 14 m s^{-1} by sunrise. (Pamperin and Stilke 1985.)

ening of the valley occurs at upper levels, as in Colorado's Gore Valley, near Vail (Fig. 2.39).

2.7.4. *Antiwind systems*

The different streams of the valley wind system (up-valley and down-valley currents) are thought to represent the lower branch of a circulation that exists between mountain and plain. Thus, for example, the up-valley current during daytime is compensated by a flow from mountain to plain above the valley ridgetops. These return circulations are rarely observed directly, except in a statistical sense (Ekhart 1944), because the compensation current is not confined to a channel like the lower branch of the circulation. Thus it is much weaker than the lower branch and is weaker than typical prevailing synoptic winds. In some cases, however, and especially in a series of experiments conducted in valleys extending radially outward from the volcanic cone of Mount Rainier, Washington, the return circulations have been observed in the upper altitudes of the valleys below ridgetop level (Buettner and Thyer 1966). In the years since these observations were taken there have been few reports of other antiwind systems.

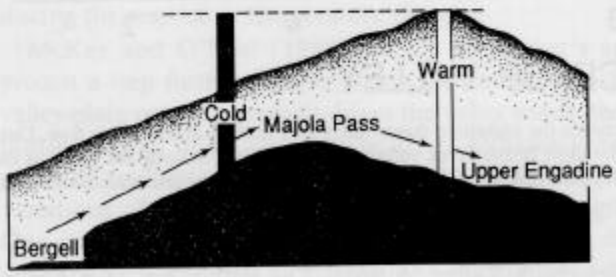

FIG. 2.36. Daytime winds in the Upper Engadine Valley blow down-valley, in apparent contradiction to theory. This wind system feature is an example of a wind system from one valley (the Bergell) streaming over a pass (Maloja Pass) into the upper reaches of another valley (Upper Engadine). The extension of the Bergell ridgeline into the Upper Engadine may produce along-valley topographic amplification factor gradients that lead to horizontal temperature gradients and the unusual winds. (Adapted from Hawkes 1947.)

2.7.5. *Tributary flows*

No effort has yet been reported in the literature to evaluate the details of tributary/main valley atmospheric interactions at valley junctions. Temperature measurements at the Ziller Valley/Inn Valley juncture show unusual warming in the main valley during daytime (Brehm 1986), which Freytag (1987) has suggested represents enhanced sinking motions compensating for the up-tributary flows (Fig. 2.40). The details of interactions at such junctures would certainly depend on the relative topography of the two valleys, the local topography at their juncture, and the detailed wind and temperature structure of the individual valley flows. It would thus be difficult to gain general knowledge from the investigation of individual cases. Nonetheless, the bulk characteristics of the individual flows have important applications for air pollution dispersion. For example, the inflow from a tributary represents, in many cases, the import of clean air into a polluted main valley atmosphere.

During nighttime, drainage currents into the broad, shallow Rhine Valley from small tributaries (Fig. 2.41) appear to maintain their identity for some distance out onto the floor of the main valley (Heldt and Höschele 1989). There is no corresponding up-tributary flow apparent in wind roses in the main valley during daytime, reflecting the influence of stability in maintaining the identity of nighttime flows. This effect is apparent, as well, in wind observations near the exit of the Inn Valley (Fig. 2.38), where an up-valley current is not present over the adjacent plain during daytime but a down-valley current is strongly in evidence during nighttime.

Tributary flows in Colorado's Brush Creek valley have been studied recently by a number of investigators (e.g., Coulter et al. 1989; Porch et al. 1989a,b). Data collected in the valley on 6 October 1984 by Neff and King (1987) suggested that shallow drainage flows in the upper drainage areas of the valley are susceptible to disruption by strong above-valley winds. Drainage flow in a tributary canyon decreased suddenly when winds above the valley accelerated to 7 m s^{-1} at 0400 MST. This was followed a half-

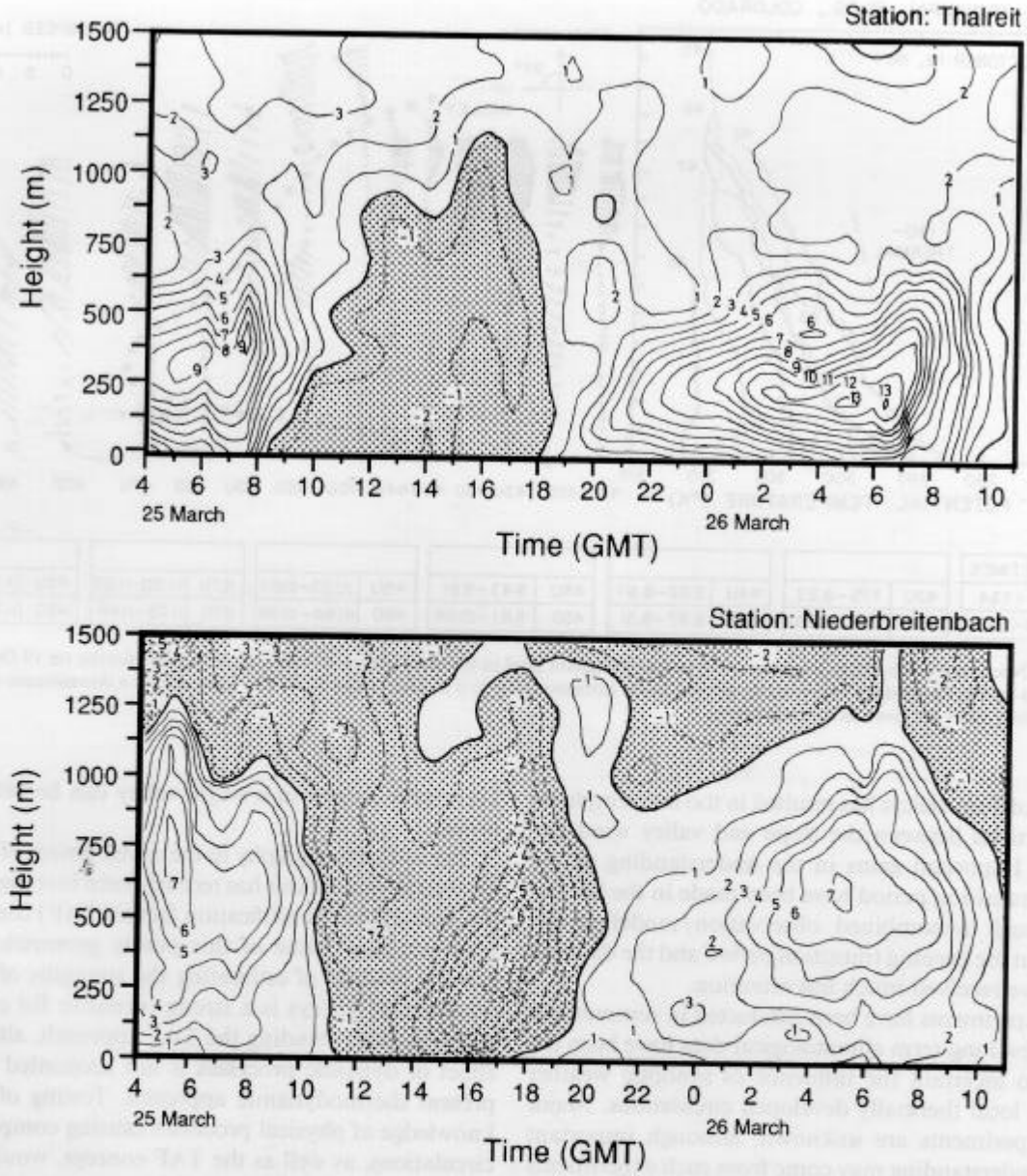

FIG. 2.38. Isopleths of along-valley wind components (m s^{-1}) at a valley station (Niederbreitenbach) and a nearby plain station (Thalreit) near the exit of the Inn Valley on 25–26 March 1982. Negative wind speeds indicate up-valley winds. (Pamperin and Stilke 1985.)

hour later by a 50% decrease in down-valley wind speeds in the main valley.

2.8. Future research

Complex terrain meteorology experiments conducted in the last decade have improved our understanding of physical processes leading to local thermally developed wind systems. The experiments have benefited from the availability of new research tools, including remote sensors, and have largely been conducted in short campaigns that have focused attention on local circulations and temperature structure evolution in simple topography during clear undisturbed weather. Much of the experimentation has been focused on drainage flows in individual valleys, largely because the low-turbulence nighttime flows can be investigated with relatively inexpensive tethered balloon measurement systems. A few experiments have investigated downslope flows on the slopes of isolated mountains, using instrumented towers. These studies have given way to investigations of nocturnal down-valley flows in simple valleys. The logistical difficulty of instrumenting

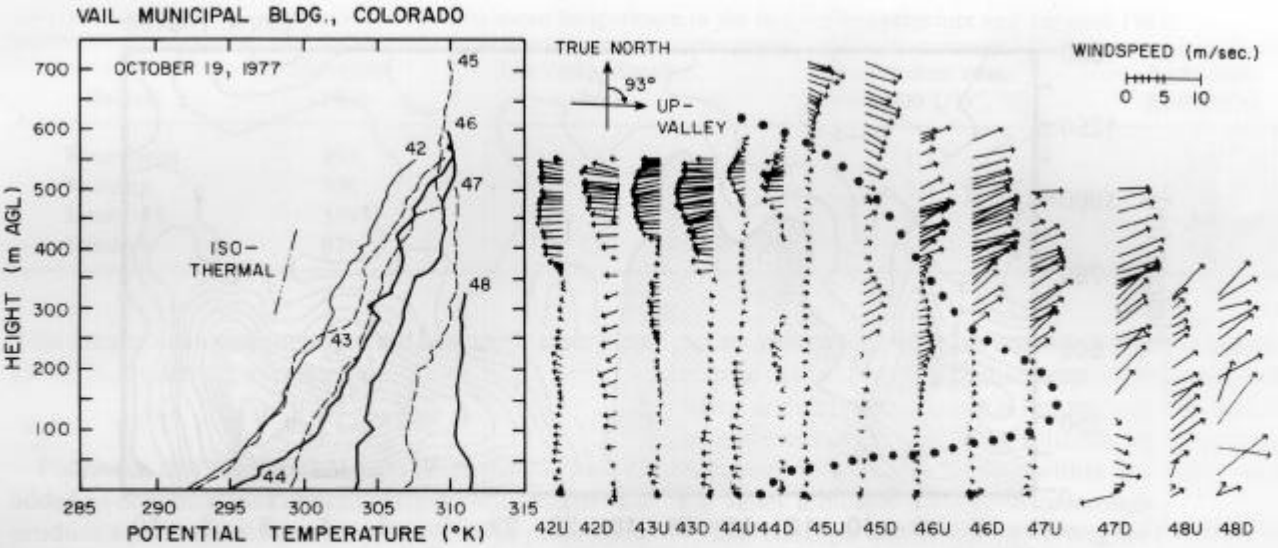

SOUNDING	TIMES												
42U	6.91–7.34	43U	7.75–8.22	44U	8.62–8.97	45U	9.43–9.81	46U	10.23–10.64	47U	11.00–11.23	48U	11.57–11.71
42D	7.34–7.60	43D	8.22–8.58	44D	8.97–9.31	45D	9.81–10.09	46D	10.64–10.99	47D	11.23–11.44	48D	11.71–11.80

FIG. 2.39. Nocturnal down-valley jet above a 400-m-deep stagnant pool in the Gore Valley at Vail, Colorado, near sunrise on 19 October 1977. The jet winds in the 700-m-deep valley occur at an altitude corresponding to a sudden widening of the valley above a downstream constriction. Profile sounding times are given in decimal hours.

the slopes of deep valleys has resulted in too little emphasis on interactions between the slope and valley wind circulations. Important gains in the understanding of the morning transition period have been made in the last decade through a combined observation/modeling approach, but the evening transition period and the daytime period have received much less attention.

Most experiments have been conducted in summer and fall, and few long-term climatological data have been developed to ascertain the influence of synoptic weather events on local thermally developed circulations. Major winter experiments are unknown, although important gains in understanding may come from such experiments because of certain surface energy budget simplifications.

The focus of most past experiments has been on the development of the wind structure. Increased emphasis now seems desirable on several boundary conditions affecting wind system development. The roles of topography, the surface energy budget, and interactions with external circulations are topics that should now receive increased emphasis. If these topics are pursued, a different experimental design may become more appropriate. Experiments, rather than focusing intensive efforts on a single valley, may need to become more *extensive,* focusing on differences between multiple valleys. In this way, for example, the influence of differing boundary conditions can be investigated and the general applicability of detailed knowledge gained in a single valley can be better determined.

The role of topography in the development of thermally developed circulations has recently been investigated using the topographic amplification factor (TAF) concept. The great practical value of this purely geometric or topographic method of estimating the strengths of wind circulations in valleys is a strong incentive for evaluating, refining, and extending the TAF approach, although the effect of dynamic processes is not accounted for in the present thermodynamic approach. Testing of our basic knowledge of physical processes causing complex terrain circulations, as well as the TAF concept, would be facilitated by extending experiments into valleys, basins, and tributaries of different size, shape, length, width, and other topographic characteristics. Topographic effects could be tested by a combined modeling/observation approach.

The topographic amplification factor can be viewed as one of a number of possible integral geometrical or topographical measures (in this case, area to volume ratios) that are relevant to meteorological investigations in complex terrain. Other such measures should prove useful in improving our understanding of complex terrain meteorology. Petkovsek (1978b, 1980), for example, has defined several topographical parameters related to the buildup and outflow of cold air pools in basins, as well as an integral measure of the susceptibility of a basin to

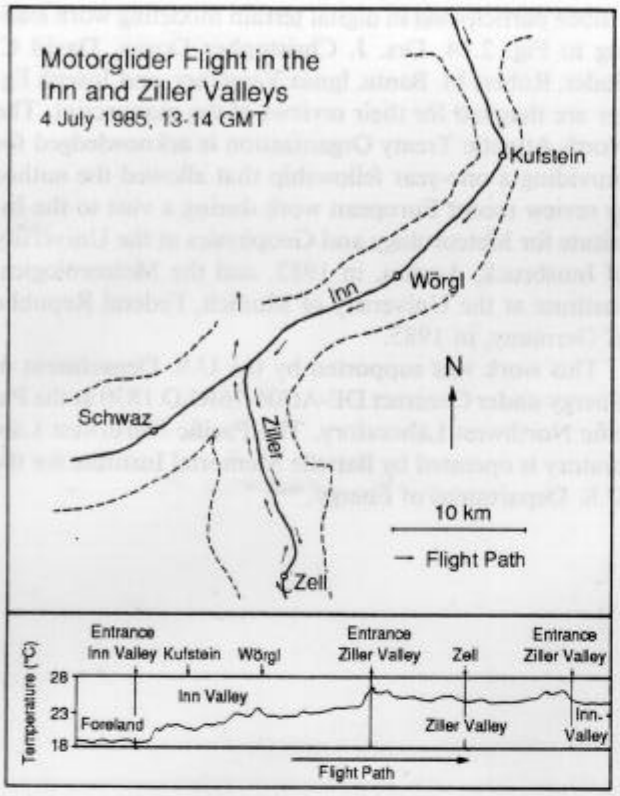

FIG. 2.40. Motorglider temperature measurements over the foreland, in the main Inn Valley, and in a major tributary valley (Ziller Valley) on 4 July 1985. Temperature increases with distance up the Inn Valley and a warm zone is observed at the exit of the Ziller Valley. The aircraft flew approximately 750 m above the ground along the flight path shown. (Brehm 1986.)

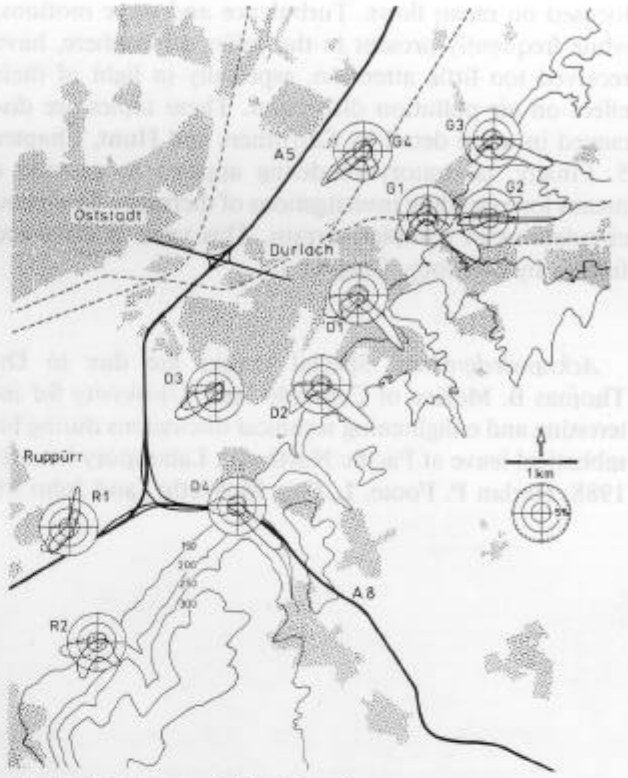

FIG. 2.41. Wind directions and speeds at the east edge of the wide, shallow, Rhine Valley near Karlsruhe, Federal Republic of Germany at 0000–0300 UTC 30 May 1979. During this moderately cloudy period, regional flows were from the southwest. Flows issuing from the tributaries maintain their identity for some distance from the tributary exits. Daytime flows (not shown) do not show a corresponding effect on the wind roses on the main valley floor. (Heldt and Höschele 1989.)

influence by upper winds. Neff and King (1987, 1988, 1989) have used other topographic parameters, such as the cross sectional area of constrictions, to investigate the effects of basin topography on local wind systems in the Geysers region in California. In another approach, Pielke and Kennedy (1980) computed the characteristic spectrum of terrain scales on a cross section of the Blue Ridge Mountains to determine the appropriate grid size for an atmospheric numerical model. Nevertheless, only a few efforts have so far been made to systematically classify terrain in ways that are relevant for meteorological investigations, although terrain has been classified for military, geomorphic, geologic, and other purposes (e.g., see Carr and Van Lopik 1962; Orgill 1981). The condensation of detailed topographical information into a few simple integral parameters that are relevant to the physics of the development of local circulations is an interesting new approach that will be facilitated by the increased availability of digital topographic databases and graphical presentation capabilities (McEwen et al. 1983; Elassal and Caruso 1983).

The role of the valley radiation and surface energy budgets in driving topographic circulations should be investigated further. Techniques and equipment should be developed so that such measurements can become a regular feature of complex terrain field experiments. Techniques are needed to make such measurements over slopes, to choose representative locations for such measurements, and to estimate spatial variations over complex terrain areas from small numbers of point measurements or from remotely sensed data.

External winds may produce more or less strong influences on the development of valley circulations. A series of carefully designed experiments could be used to determine the mechanisms by which these influences are felt, and climatological studies would prove helpful in quantifying their effects on valley meteorology over time.

Most valley meteorology investigations to date have

focused on mean flows. Turbulence and wave motions, while frequently present in the valley atmosphere, have received too little attention, especially in light of their effect on air pollution dispersion. These topics are discussed in more detail by Carruthers and Hunt, Chapter 5. Finally, laboratory modeling appears to provide a means for extending investigations of thermally developed circulations in complex terrain. This topic is discussed further by Meroney, Chapter 7.

Acknowledgments. Special thanks are due to Dr. Thomas B. McKee of Colorado State University for interesting and enlightening technical discussions during his sabbatical leave at Pacific Northwest Laboratory in early 1988. Harlan P. Foote, L. Guy McWethy, and John M. Hubbe participated in digital terrain modeling work leading to Fig. 2.14. Drs. J. Christopher Doran, David C. Bader, Robert M. Banta, Ignaz Vergeiner, and Joseph Egger are thanked for their reviews of the manuscript. The North Atlantic Treaty Organization is acknowledged for providing a one-year fellowship that allowed the author to review recent European work during a visit to the Institute for Meteorology and Geophysics at the University of Innsbruck, Austria, in 1983, and the Meteorological Institute at the University of Munich, Federal Republic of Germany, in 1985.

This work was supported by the U.S. Department of Energy under Contract DE-AC06-76RLO 1830 at the Pacific Northwest Laboratory. The Pacific Northwest Laboratory is operated by Battelle Memorial Institute for the U.S. Department of Energy.

from

Whiteman, C. D., 1990: Observations of thermally developed wind systems in mountainous terrain. Chapter 2 in Atmospheric Processes Over Complex Terrain (W. Blumen, Ed.), *Meteorological Monographs*, **23**, no. 45. American Meteorological Society, Boston, Massachusetts, 5-42.